Final Report
on the project NKFI-116465 entitled
“Synthesis and characterization of smart fluorescent polymers”
(2016.01.01.-2020.03-31.)

Debrecen, 2020

Table of Contents

I. Brief summary of the results....3

II. MICAN, a new fluorophore for vital and non-vital staining of human cells....7

III. Antifungal activity of an original amino-isocyanonaphthalene (ICAN) compound....10

IV. Isocyanonaphthalenes as selective ratiometric probes for Hg(II)....13

V. Acrylated isocyanonaphthalene based solvatochromic click reagent....16

VI. Acrylated isocyanonaphthalenes for staining living plant cell....19

VII. Application of solvatochromic isocyanonaphthalene dyes in silver(I) detection and backgroundreduction in biolabelling....23

VIII. Influence of gold nanoparticles on the fluorescence property of ACAIN....27

IX. Effect of the substitution position on the electronic and solvatochromic properties of ICAN)s....28

X. Amino-isocyanoacridines: novel, tunable solvatochromic fluorophores as physiological pH probes....30

I. Brief summary of the results

During the four-year period of this project, we focused our attention on the preparation, characterization and application of the members of a novel solvatochromic dye family called ICANs (amino-isocyanonaphthalenes) developed by our research group [1]. We introduced a very effective group of solvatochromic molecules, where the amino group was the donor and the isocyano group was the acceptor both located on an aromatic ring. The first member of this group was the 1-amino-5-isocyanonaphthalene (1,5-ICAN) [1]. The emission maximum of 1,5-ICAN falls in almost every solvent in the visible region of the spectrum, and batochromically shifted with increasing solvent polarity (409 nm in hexane to 513 nm in water). The fluorescent properties of 1,5-ICAN were further enhanced by the alkylation of the amino group, namely mono- and dialkylated derivatives of 1,5-ICAN (1,5-MICAN and 1,5-diMICAN, respectively) were also synthesized. It was confirmed that 1,5-ICAN and especially its N-methylamino derivative 1,5-MICAN could serve as a nonselective fluorescent dye capable to stain cellular structures of fixed, living, damaged and dead cells [2]. Interestingly, during our cell staining experiments, we also recognized that some 1,5-ICAN derivatives especially 1,5-diMICAN showed significant antifungal activity [3]. The in vitro antifungal activity against reference strains of clinically important *Candida* species was confirmed and 1,5-diMICAN was found to be effective against intrinsically fluconazole resistant *Candida krusei* isolates, too.

We also demonstrated that 1,5-ICAN enables the selective detection of Hg(II)-ions (with a limit of quantification $\leq$ 17 nM, and a limit of detection $\leq$ 6nM) and at the same time is able to indicate the presence of Ag(I)-ions [4]. To the best of our knowledge, 1,5-ICAN is the lowest molecular weight dye reported for ratiometric fluorescent Hg(II) detection in water, so far.

All the 1,5-ICAN derivatives synthesized so far contained no reactive group by which any selective labeling could be performed. Therefore, in order to enable and extend our ICAN family for biolabeling we introduce an acrylate group into the 1,5-ICAN moiety [5]. Thus, a novel member of the ICAN family, namely 1-(2-acryloyloxy-3-chloro-prop-1-yl)-amino-5-isocyanonaphthalene (ACAIN) was synthesized. It was shown that ACAIN quantitatively and rapidly reacts with simple thiols in a thiol-ene click reaction and the hydrothiolation reaction is accompanied by a 1.5-19 fold increase in fluorescence intensity depending on the solvent used owing to the saturation of the acrylic group. The quantum yield and reactivity of the molecules were found to be largely dependent on the substituent of the acryl moiety. The

biolabeling properties were modeled using model compounds such as a cysteine containing tripeptide and BSA.

The biolebeling property of ACAIN was also tested in living cells [6]. We demonstrated that ACAIN preferentially label tonoplasts in living Arabidopsis and tobacco (Nicotiana tabacum SR1) cells while preserving the dynamics of vacuolar structures. ACAIN proved also to be suitable for the labeling and detection of specific (cysteine-rich, hydrophobic) proteins from crude cell protein extracts. It was demonstrated that ACAIN can also be used for the selective detection and quantification of Ag(I)-ions in aqueous media and the fluorescence switch-off can lead to a significant contrast enhancement in biolabeling applications as shown on fixated HaCat cells [7].

ACAIN were also copolymerized with diurethane-methacrylate (UDMA) and isodecyl methacrylate (IDA) comonomers in the presence of dodecanethiol-functionalized gold and SiO_2 nanoparticles [8]. This way, a new polymer nanocomposite was obtained. It was also shown that the addition of SiO_2 nanoparticles enhances the fluorescent intensity of ACAIN by 1.5 times in the 450-550 nm spectral range. Furthermore, an additional up to 4.5-fold fluorescence enhancement was observed when Au-nanoparticles were added to this nanocomposite in a rather low (0.12 wt %) concentration.

To vary the fluorescence properties of the ICAN fluorophore family we focused our attention to the synthesis of ICAN derivatives in which the donor amino and the acceptor isocyano groups are located in different positions [9]. With these variations in the structure we were hoping that we would obtain deeper insight into the fluorescence properties of these ICAN derivatives, on one hand, and allow us a comprehensive comparison of the corresponding properties of these molecules, on the other. Thus, 1,4- and 2,6-ICAN were synthesized in addition to 1,5-ICAN. Indeed, it was found that the positions of the donor and the acceptor groups in these naphthalene derivatives greatly influence the Stokes and solvatochromic shifts, which decrease in the following order: 1,5-ICAN > 2,6-ICAN > 1,4-ICAN. According to high-level quantum chemical calculations, this order is well correlated with the charge transfer character of these compounds upon excitation. Furthermore, unlike 1,5-ICAN, the 1,4-ICAN and 2,6-ICAN isomers showed relatively high quantum yields in water.

In a next series of experiments, the aromatic moiety was modified to obtain 3-amino-6-isocyanoacridine (ICAAc), and with further reactions of ICAAc with CH_3I we were able to synthesize 3-N-methylamino-6-isocyanoacridine (monoMICAAc) and 3-N,N-dimethylamino-6-isocyanoacridine (diMICAAc) derivatives [10]. These ICAAcs derivatives proved to be a multifunctional acridine orange (AO) type dye family with a number of additional favorable

properties such as enhanced solvatochromic emission range, low quantum yields (Φ_F = 2.9–0.4%) in water, reduced basicity (pK_a = 7.05–7.58), and their optical behavior could be fine-tuned by complexation with Ag(I) ions, too. In addition, ICAAcs can be applied as stable pH-probes with great precision (2–3% error) in the physiological pH range of 6–8 using UV-vis and fluorescence detection. All three dyes are well-applicable with conventional epifluorescence imaging. Furthermore, at the blue excitation, diMICAAc is optimally suited as a whole-cell probe for both the conventional microscopic and the laser-illumination studies, like flow- and imaging cytometric, or confocal laser-scanning microscopic examinations.

Our research on these fluorophores led to two additional results. The ACAIN has a free hydroxyl group, which is theoretically capable of reacting with diisocyanates. This way, we thought of this reaction as a simple reaction route to extend and improve the fluorescent properties of ACAIN. Albeit, in this case, the reaction path outlined here did not yield the desired reaction product(s), it, however, led to the initiation of two subsequent studies on the reactions of alcohols with diisocyanates [11,12]. The second inspeiration came from the evaluation of complicated MS spectra such as those obtained for the complex reaction mixture of ICAN derivatives or other compounds e.g. copolymers. To easy the analysis of such complex MS spectra an algorithm called Mass-remainder Analysis (MARA) was developed and published [13].

References

1. Rácz, D.; Nagy, M.; Mándi, A.; Zsuga, M.; Kéki, S.: Solvatochromic properties of a new isocyanonaphthalene based fluorophore, *Journal of Photochemistry and Photobiology A: Chemistry*, **270**, 19-37 (2013)
2. Nagy, Z.; Nagy, M.; Kiss, A.; Rácz, D., Barna, B., Könczöl, P., Bankó, C.; Bacsó, Z., Kéki, S.; Banfalvi, G.; Szemán-Nagy, G.: MICAN, a new fluorophore for vital and non-vital staining of human cells, *Toxicology in Vitro,* **48**, 137-145 (2018)
3. Nagy, M.; Szemán-Nagy, G.; Kiss, A.; Nagy, Z.L.; Tálas, L.; Rácz, D.; Majoros, L.; Tóth, Z.; Szigeti, Z.M.; Pócsi, I.; Kéki, S.: Antifungal activity of an original amino-isocyanonaphthalene (ICAN) compound family: Promising broad spectrum antifungals, *Molecules*, **25(4),** Article number 903 (12 page) (2020)
4. Nagy, M.; Kovács, S.L.; Nagy, T.; Rácz, D.; Zsuga, M.; Kéki, S.: Isocyanonaphthalenes as extremely low molecular weight, selective, ratiometric fluorescent probes for Mercury(II), *Talanta*, **201**, 165-173 (2019)
5. Nagy, M.; Rácz, D.; Nagy, Z.L.; Nagy, T.; Fehér, P.P.; Purgel, M.; Zsuga, M.; Kéki, S.: An acrylated isocyanonaphthalene based solvatochromic click reagent: Optical and biolabeling properties and quantum chemical modeling, *Dyes and Pigments*, **133**, (445-457) (2016)

6. Nagy, M., Kéki, S., Rácz, D., Mathur, J., Vereb, G., Garda, T., M-Hamvas, M., Chaumont, F., Bóka, K., Böddi, B., Freytag, C., Vasas, G., Máthé, C.: Novel fluorochromes label tonoplast in living plant cells and reveal changes in vacuolar organization after treatment with protein phosphatase inhibitors, *Protoplasma*, **255(3),** 829-839 (2018)

7. Nagy, M.; Rácz, D.; Nagy, Zs.L.; Fehér, P.P. Kalmár, J. Fábián, I.; Kiss, A. Zsuga, M.; Kéki, S.: Solvatochromic isocyanonaphthalene dyes as ligands for silver(I) complexes, their applicability in silver(I) detection and background reduction in biolabelling, *Sensors and Actuators B: Chemical,* **255**, 2555-2567 (2018)

8. Burunkova, J.; Kéki, S.; Veniaminov, A.; Nagy, M.; Daróczi, L.; Kökényesi, S.: Influence of Gold Nanoparticles on the Luminescence of an Acrylated Isocyanonaphthalene Derivative, *Advances in Condensed Matter Physics*, Article Number: 8084659 (2019)

9. Kovács, S.L.; Nagy, M.; Fehér, P.P.; Zsuga, M.; Kéki, S.: Effect of the Substitution Position on the Electronic and Solvatochromic Properties of Isocyanoaminonaphthalene (ICAN) Fluorophores, *Molecules*, **24**, Article Number: 2434 (2019)

10. Nagy, M.; Rácz, D.; Nagy, Zs.L.; Fehér, P.P.; Kovács, S.L.; Bankó, Cs.; Bacsó, Zs.; Kiss, A., Zsuga, M.; Kéki, S.: Amino-isocyanoacridines: Novel, Tunable Solvatochromic Fluorophores as Physiological pH Probes, *Scientific Reports*, **9**, Article Number: 8250 (2019)

11. Nagy, L.; Nagy, T.; Kuki, Á., Oláh, R.; Lakatos, Cs.; Zsuga, M.; Kéki, S:: Reactions of 2,6-Toluene Diisocyanate with Alcohols: Kinetic Studies in the Absence and Presence of Catalysts, *Chemistryselect*, **2,** 11302-11306 (2017)

12. Nagy, L.; Nagy, T.; Kuki, Á.; Purgel, M.; Zsuga, M.; Kéki, S.: Kinetics of Uncatalyzed Reactions of 2,4′- and 4,4′-Diphenylmethane-Diisocyanate with Primary and Secondary Alcohols, *International Journal of Chemical Kinetics*, **49**, 643-655, (2017)

13. Nagy, T., Kuki, Á., Zsuga, M., Kéki, S.: Mass-Remainder Analysis (MARA): A New Data Mining Tool for Copolymer Characterization, *Analytical Chemistry*, **90,** 3892-3897 (2018)

II. MICAN, a new fluorophore for vital and non-vital staining of human cells

As an application of our new ICAN fluorophore family (amino-isocyanonaphthalenes) we tested the members of ICANs as a vital and non-vital dye. According to the results of our experiments, the 1-N-monomethylamino-5-isocyanonaphthalene (MICAN) was chosen over the other ICAN derivatives because of its low reactivity relative to other ICAN members of this fluorophore family. The slow metabolism of MICAN in eukaryotic cells was accounted for by the presence of the methylamino group that provided higher stability to perform long-term experiments *versus* other derivatives of ICANs. The motivation of cell staining was a growing interest in new fluorescent dyes that are taken up by cells without damaging them. In this research we focused on (i) the uptake of MICAN by the extracellular matrix, of HaCaT cells (ii) determination of the lowest toxic concentration, where cells can still divide without detectable signs of apoptosis or necrosis and (iii) determination of sufficient fluorescence signals for the detection of the inner cell structure.

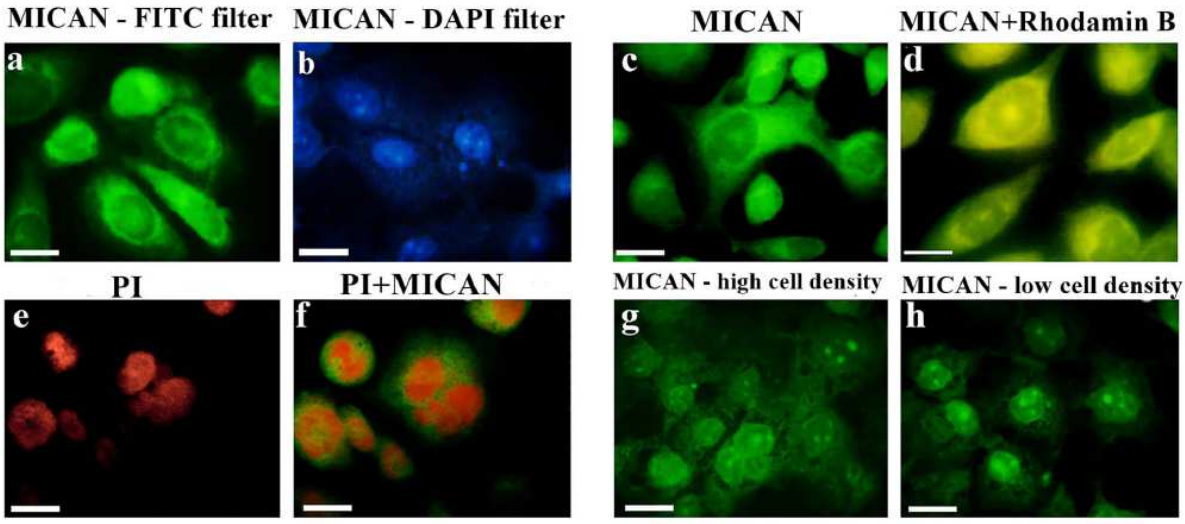

Figure 1. Staining and co-staining of HaCaT cells with MICAN under different conditions. Cells were fixed with 4% PFA for 10 min, dehydrated then stained with MICAN as described in the Methods. Fluorescence microscopy with a) FITC filter, b) with DAPI filter. Bars, 50 μm each at 100× magnification. c) Staining of cells with MICAN, and d) combined rhodamin B and MICAN staining. Bars 50 μm each, at 63× magnification. e) PI staining (red), f) PI staining followed by additional staining with MICAN (external green color). Bars 50 μm each, 63×. g) In situ microscopic examination of HaCaT cells with MICAN, co-incubated for 24 h and fixed with 4% PFA for 10 min. Fluorescence microscopy of MICAN with g) FITC filter, h) with DAPI filter. Bars, 50 μm each at 100× magnification.

Fig. 1. demonstrates the staining pattern of MICAN under different staining conditions. To test the fluorescent properties of MICAN, FITC and DAPI filters were used for fluorescence microscopy. Microscopic images were taken with DAPI filter to prove that MICAN as a fluorescent dye acted similarly to DAPI and could be a useful stain for fluorescence microscopy either with FITC (Fig. 3a) or DAPI (Fig. 3b) filters. Higher accumulation of the fluorescent MICAN was observed around the outer surface of the cell membrane and moderate staining of the nucleus, but not to its double membrane, pointing to the binding of MICAN to proteins.

Time-lapse laser-scanning microscopy at low excitation energy was used to collect 80 images within a 5 hour period as shown in Fig. 2. The progress of slow cellular death was followed by parallel propilium iodide (PI) staining. No cross-talk effect was found between the two fluorophore during the experiment. Analysis of the acquired image sequences indicate low staining background and insignificant photobleaching of the MICAN resulting in a high signal/noise ratio within the experimental interval as shown on the linear plots in Fig. 3. It is to be noted that no phototoxicity was observed during the experiment.

As a conclusion of our work it can be astablished that the fluorophore MICAN molecule is applicable in cell staining practice both as a nonvital, and a vital dye. MICAN showed characteristic binding to cytoplasmic proteins and a slight selectivity to spots of proteins in the nuclear heterochromatin. The compound is well tolerated by human cell cultures between 0.5 and 10 μg/ml concentrations. Furthermore, there is sufficient intensity for fluorescence imaging in the nontoxic range between concentrations of 0.5 and 10 μg/ml. The function of the cells is affected at higher concentrations when MICAN binds to proteins of the cell and modifies their function. Visible torsions in cells were observed in the 20–30 μg/ml MICAN concentration range. Nonspecific

MICAN staining of cellular proteins allowed the long term tracking of subcellular processes by fluorescent time-lapse microscopy. According to fluorescent time-lapse microscopy investigations, MICAN showed spectral separation from PI offering a possible co-application of the two dyes. Within a five-hour long experiment no photobleaching was observed. Due to the high quantum efficiency of MICAN, the intensity of the excitatory fluorescent light could be reduced significantly, and minimized the major problem, namely the phototoxicity of time-lapse microscopy. Advantages of MICAN as a “Live-or-Die” dye can be summarized as:

- Minimal invasiveness: Low toxicity within the application range
- Stability: Minimal or negligible photobleaching
- Efficiency: High quantum-efficiency helping to reduce phototoxicity

due excitation

- Affordable: Lower cost than commercial stains
- Choice: 8 bright colors across the spectrum
- Non-specific: Staining of live and dead cells
- Fixable: No loss of brightness after fixation
- Versatile: Applicable both for light and fluorescence microscopy

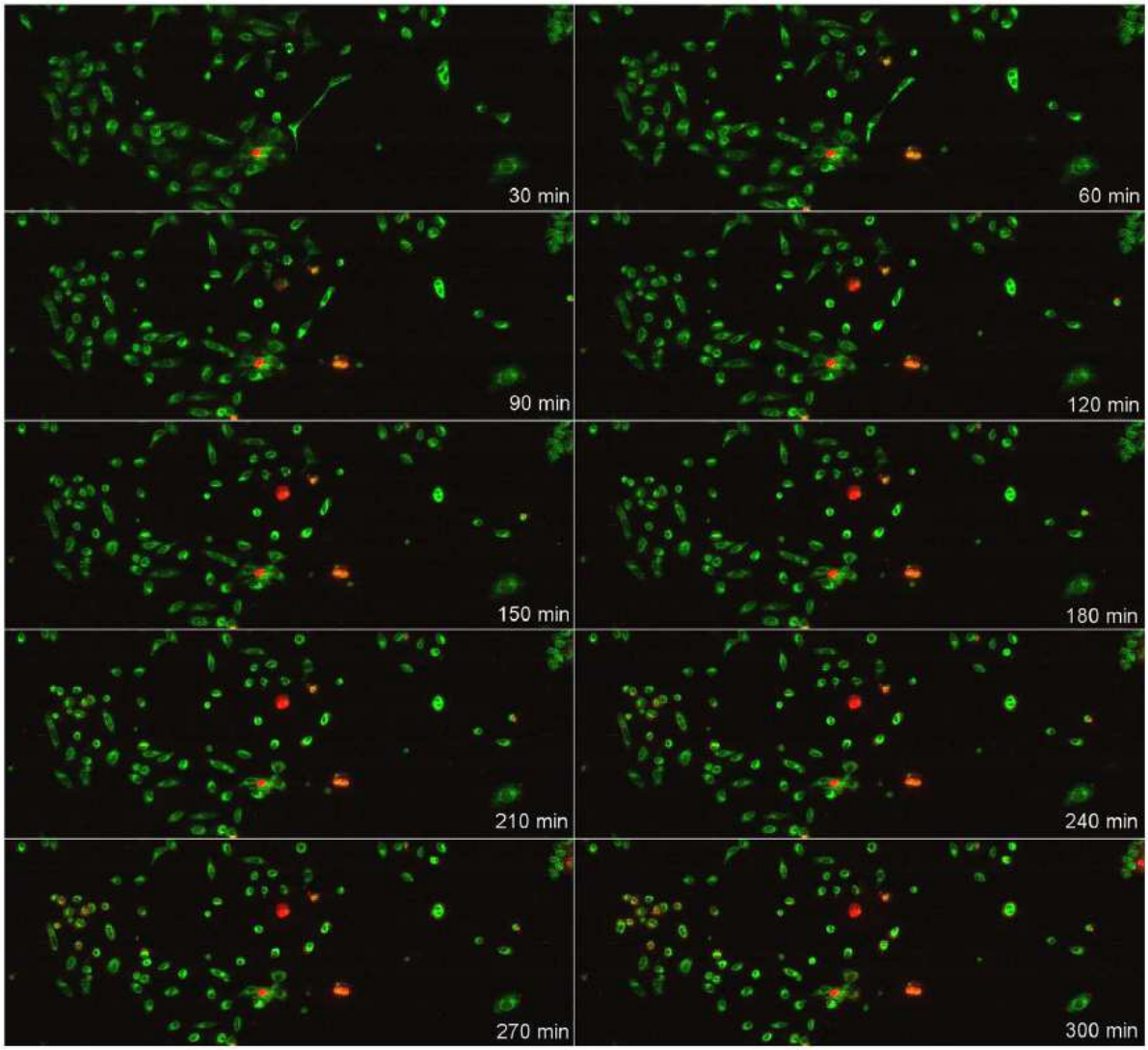

Figure 2. Fluorescent time-lapse image sequence of temperature-induced death of HaCat cells. Cells were kept at room temperature during the 5 h period of time-lapse imaging. Laser scanning microscopy of HaCaT cells in the presence of 0.5 µg/ml MICA concentration. Live cells were seen in green and cell death tested by propidium iodide (PI, 5 µg/ml) at room temperature for 300 min. MICAN and PI fluorescent dyes were applied simultaneously. MICAN was excited at 405 nm by a violet solid-state laser (0.71mW at turret), while PI was excited at 488 nm by a blue diode laser (turret intensity: 0.68 mW). Fluorescence emission was detected with a band-pass filter at 530 ± 30 nm and with a long-pass filter above 650 nm, respectively.

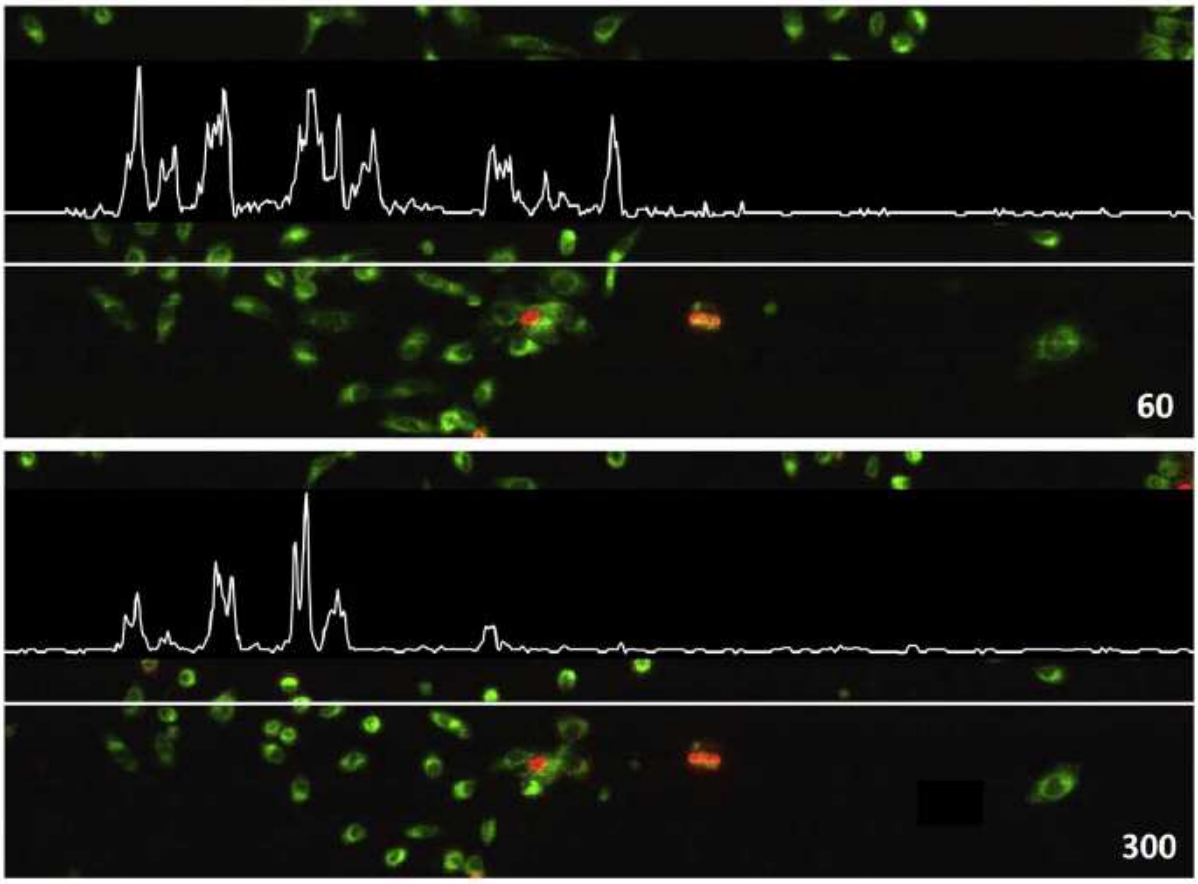

Figure 3. Linear plot profile of fluorescent images acquired at 60 and 300 min. White lines indicate pixels with green channel intensity measured and represented at the graphs above.

III. Antifungal activity of an original amino-isocyanonaphthalene (ICAN) compound

Members of the Candida genus are part of the healthy human microbiome and can be found in the oral cavity, gastrointestinal and urogenital tract, however, as opportunistic pathogens, these yeasts can cause a wide variety of diseases ranging from superficial infections to life threatening invasive candidiasis. The aims of this study were to test the antifungal activity of 1-amino-5-isocyanonaphthalene (ICAN) and its derivatives on different *Candida* species in vitro, and to test the most effective agent in vivo, in a murine model of invasive candidiasis. This observation can lead to the development of a new compound family, which can rival the currently approved drug classes or even top them in several fields of application. It should be noted, however, that this investigation focused only on the 1,5-ICAN derivatives, whereas ICANs are easy to modify and even the slightest change in the relative substitution position of the amino and isonitrile groups on the naphthalene ring can result in a completely different behavior.

ICAN has 3 key moieties, namely the amino, naphthalene and isonitrile. To find out which ones of them are essential for the antifungal activity and to design more efficient derivatives, comparative studies were carried out, where one of the moieties was exchanged or eliminated. The modification/synthetic strategy is summarized in Fig. 4. All ICAN derivatives were tested against *Candida albicans*, *Candida krusei* and *Candida parapsilosis*.

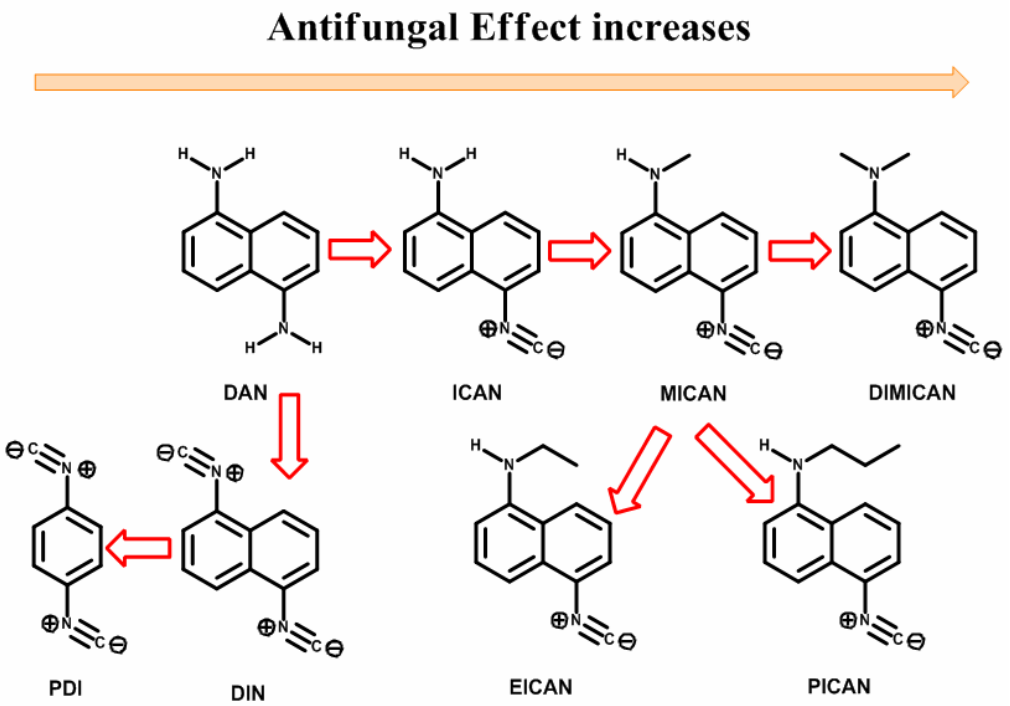

Figure 4. The development strategy for the most effective 1-amino-5-isocyanonaphthalene (ICAN) derivative.

Based on our results we concluded that even the simplest amino-isocyanonaphthalene molecule ICAN has good antifungal effect with minimum inhibitory concentration for total inhibition (MIC_{TI}) values between 0.6–5 μg/mL. The starting compound 1,5-diaminonaphthalene (DAN) from which ICAN derivatives were synthesized proved to be completely ineffective against *Candida* (MIC_{TI}> 100 μg/mL), therefore, we can conclude that the isonitrile group is essential for the antifungal effect. Next the free amino group of ICAN was converted to isonitrile resulting 1,5-diisocyanonaphthalene (DIN), which showed similar (or higher) antifungal activity (MIC_{TI} = 0.6 μg/mL) compared to that of ICAN. However, the largely nonpolar and rigid aromatic structure of DIN significantly limits its solubility in polar solvents, such as water. The naphthalene core of DIN was exchanged to phenylene to obtain 1,4-phenylenediisocyanide (PDI). In contrast to DIN, PDI proved to be completely ineffective (MIC_{TI} > 100 μg/mL), which means that the naphthalene moiety is also essential for the antifungal activity. To increase the efficiency of ICAN derivatives, the substitution of the

amino group followed. The alkylation of the amino group increases the dipolarity of the molecules, however at the same time it reduces their ability to form H-bonding as an H-bond donor. Monomethylation (MICAN) led to lowered MIC_{TI} values (0.75–1.25 μg/mL), however the use of longer alkyl chains, such as ethyl and propyl (EICAN and PICAN) proved to be not so effective (MIC_{TI} = 1.25–2.5 μg/mL and 1.75–2.5 μg/mL, respectively), maybe due to steric hinderance. The lowest MIC values were obtained in the case of DIMICAN (partial (50 %) inhibition) $MIC_{PI} \leq 0.04$ μg/mL and MIC_{TI} = 0.3–0.6 μg/mL), the dimethylated ICAN derivative. It should be noted that the MICs did not vary significantly for most of the compounds under investigation, only in the case of ICAN was a broader range observed (9-fold variation for ICAN (MIC = 0.6–5 μg/mL). For further tests we chose one of the most effective ICAN derivative, DIMICAN which has no cytotoxic effect [15,20]. To test the "real life" behavior of DIMICAN it was tested for *in vitro* susceptibility against clinical isolates collected from patients at the Clinics of the University of Debrecen.

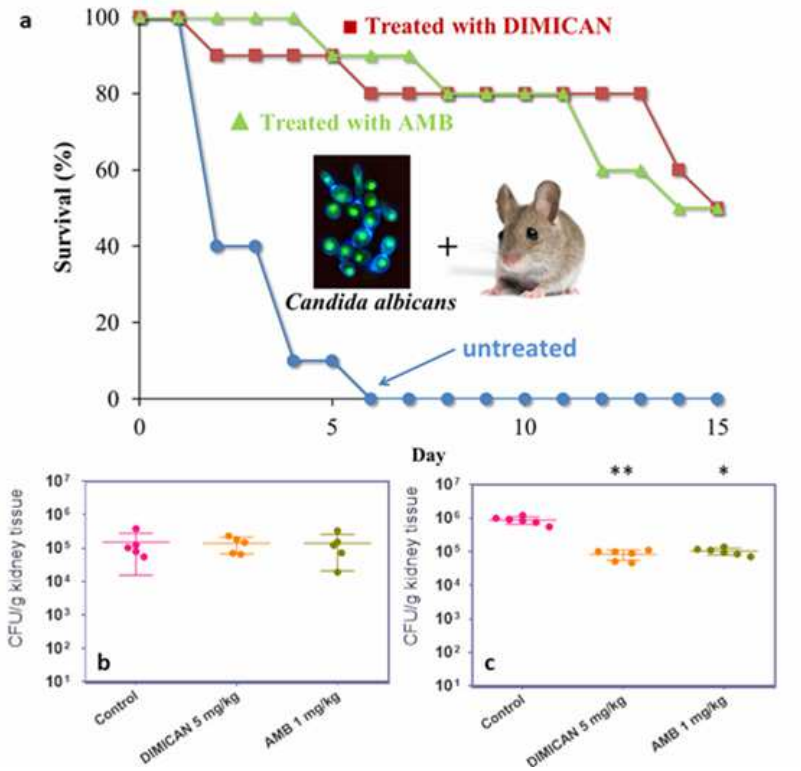

Figure 5. *In vivo* antifungal activity results for DIMICAN against *Candida albicans* 3666 isolate. (a) Survival curves of mice infected with *Candida albicans* groups n = 10. (b) Kidney tissue burden of immunosuppressed mice infected by *Candida albicans* 3666 isolate, two days after infection. (c) Six days after infection ($p < 0.05$ (*); $p < 0.001$ (**)).

Accordingly, the in vivo applicability of DIMICAN was tested on immunosuppressed mice and control experiments were also conducted with amphotericin B. In the model of acute invasive candidiasis, neutropenic mice were infected intravenously with *C. albicans* 3666

isolate (3 x 10^4 colony-forming unit (cfu)/mouse) to establish an acute infection, and all untreated control animals died within six days. DIMICAN (5 mg/kg) prolonged the survival period of animals compared with the survival period of non-treated infected controls, $P < 0.05$; 80 versus 0% survivors at day 7 post infection. Results of fungal burden in kidney revealed that six days after infection AMB and DIMICAN were effcient against Candida isolate: $p < 0.05$ (AMB); $p < 0.001$ (DIMICAN). Based on these results and the easy and versatile modification of the ICANs we hope that they have the potential to become an effective clinical lead compound family against pathogenic fungi. As potential lead compounds, ICANs, meet one or more criteria of commercial use, such as low cost, easy preparation and good chemical stability, for example after extensive toxicity and time-kill studies may be used as antimycotic coatings on medical tubes and/or devices. This simple, cheap, nontoxic and easy to prepare compound family would allow not only human treatment, but at the same time could be used as disinfectants and/or coating which is vital against the spread of highly virulent Candida strains.

IV. Isocyanonaphthalenes as selective ratiometric probes for Hg(II)

Owing to the presence of both amino and isocyano group in the 1-amino-5-isocyanonaphthalene derivatives (ICANs) we performed a series of complexation experiments of ICANs in the presence of different metal ion in various solvent and solvent mixtures. During these experiments we realized that ICANs preferred some metals ions over others for comlexation (as it, partly, was expected). Based on these experiments, ICAN and its monomethylated-(MICAN) and dimethylated derivatives (DIMICAN) turned out to be highly sensitive ratiometric fluorescent sensors for Hg(II) in aqueous solutions. Owing to its easy to preparation through a single step reaction from 1,5-diaminonaphthalene, ICAN is the simplest, lowest molecular weight fluorophore reported for this purpose until now. Its simple structure and nontoxic nature is favorable for commercial applications. The behavior of the ICAN derivatives was investigated in water in the presence of 23 common metal ions and 13 simple and complex anions, but significant spectral shift of the emission maximum happened only in the case of Hg(II) and Ag(I) as shown in Fig. 6.

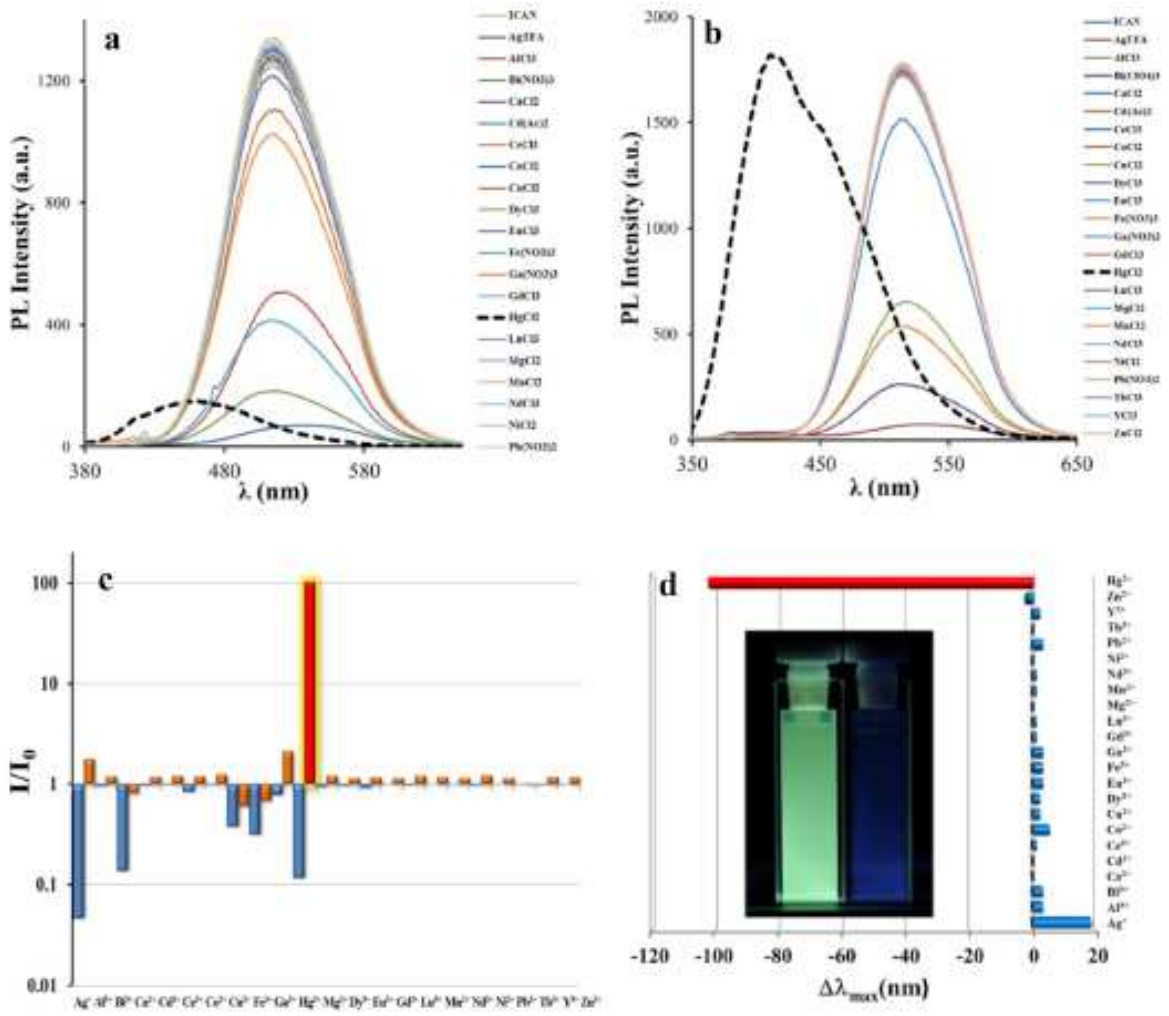

Figure 6. The spectral changes of ICAN in the presence of common metal ions. a) emission spectra recorded at λ_{ex}=365 nm. b) at λ_{ex}=337 nm. The dashed lines belong to spectra recorded in the presence of Hg^{2+}. c) intensity ratio of pure ICAN (I_0) and after the addition of ions (I) measured at 513 nm (blue bars) and at 406 nm (orange bars) d) shift of the emission maximum. The effect of Hg^{2+} is highlighted in red. The inset picture shows the aqueous solution of ICAN before (left) and after (right) the addition of Hg^{2+} under λ=365 nm UV light.(Water:MeCN, 96:4 v/v, T=20 °C, [ICAN]=4.75×10^{-5} M, [$Metal^{n+}$]=1.70×10^{-4} M).

The addition of 3 molar equivalent Hg^{2+} resulted a hypsochromic shift of 107, 112 and 94 nm for ICAN, MICAN and DIMICAN, respectively. This shift is attributed to the appearance of a new diamine emission peak, which is the result of the chemical reaction of Hg^{2+} with the isocyano moiety of the ICAN derivatives. The formation of the diamines (DAN) was revealed by both fluorimetric and ESI-MS methods (Fig.7.). Fluorescence titrations with $HgCl_2$ showed 1:1 stoichiometry for the reaction of ICANs (Fig.7.). In contrast, the addition of the same amount of Ag^+ yielded a 20 nm and 23 nm bathochromic shift for ICAN and DIMICAN, which can be attributed to 1:1 complex formation of the isocyano group with Ag^+.

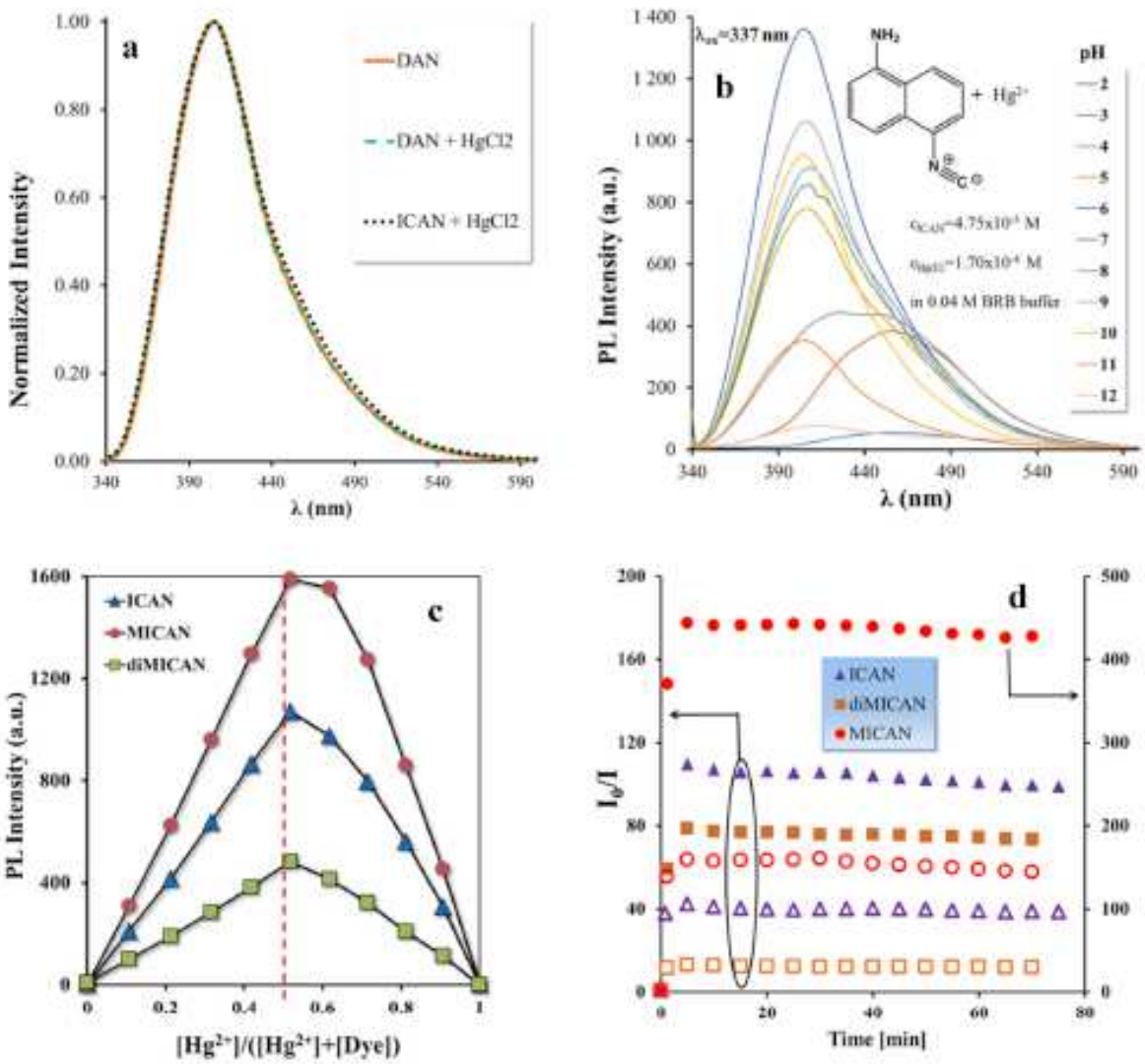

Figure 7. (a) The emission spectra of DAN (1,5-dimethylamino-naphthalene), DAN+ $HgCl_2$ and ICAN+$HgCl_2$. (b) The pH dependence of the reaction of ICAN with $HgCl_2$. (c) Job-plot for ICAN, MICAN and diMICAN. (d) Response time and stability for ICANs:Hg^{2+} 1:1 (n/n) (full marks) and 1:0.1 n/n (empty marks).

This simultaneous complexation and reduction reaction of the isocyano group enables for the same dye to detect Hg^{2+} even in the presence of large excess of Ag^{+}. However, in the absence of Hg^{2+}, the presence of Ag^{+} could be detected based on its strong quenching effect along with the bathochromic shift of the ICAN peak, which are only characteristic for Ag^{+}. We also recognized that because the Hg^{2+} detection is based on the formation of naphthalene diamines, the aqueous solution must be buffered (pH=6–10) to hinder the formation of protonated species, which lowers the sensitivity. The intensity of the amine peak ($\lambda_{em,amine}$=406, 408 and 420 nm for ICAN, MICAN and diMICAN, respectively) and their intensity ratios formed using the position of the original emission maximum ($\lambda_{em,dye}$=513, 520 and 513 nm for ICAN,

MICAN and DIMICAN, respectively) were found to be a linear function of Hg^{2+} concentration in the range of 170 nM-50 μM. The limit of detection (LOD) and limit of quantitation (LOQ) for the method was determined using the ratiometric calibration curve in the low Hg^{2+} concentration region and were found to be LOD < 6 nM and LOQ < 17 nM. Slight interference was found in the case of Fe^{3+} and Bi^{3+}, and a more pronounced interference in the case of Cu^{2+}, but only when these ions were in multiple excess compared to Hg^{2+}. The practical applicability of the method was demonstrated on freshly prepared dental amalgam.

V. Acrylated isocyanonaphthalene based solvatochromic click reagent

In order to obtain reactive ICAN derivatives acryl, methacryl and chloroacryl moieties using epichlorohydrin as spacer were introduced on ICAN. Thus, 1-(2-acryloyloxy-3-chloro-prop-1-yl)-amino-5-isocyanonaphthalene (ACAIN), 1-(2-methacryloyloxy-3-chloroprop-1-yl)-amino-5-isocyanonaphthalene (MACAIN) and (2-chloroacryloyloxy-3-chloroprop-1-yl)-amino-5-isocyanonaphthalene (CACAIN) were prepared as shown in Scheme 1.

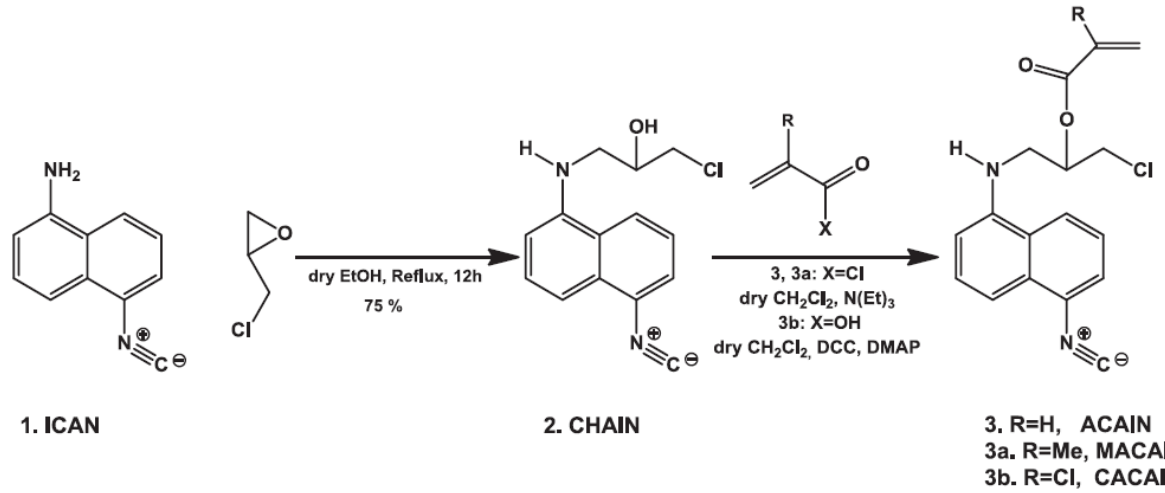

Scheme 1. Synthesis of 1-(3-chloro-2-hydroxyprop-1-yl)-amino-5-isocyanonaphthalene (2, CHAIN), 1-(2-acryloyloxy-3-chloro-prop-1-yl)-amino-5-isocyanonaphthalene (3, ACAIN), 1-N-(2-methacryloyloxy-3-chloroprop-1-yl)-amino-5-isocyanonaphthalene (3a, MACAIN) and (2-chloroacryloyloxy-3-chloroprop-1-yl)-amino-5-isocyanonaphthalene (3b, CACAIN).

All three compounds exhibited real solvatochromic behavior ($\Delta\lambda_{em}$~100 nm) which could be quantitatively described by the Catalan model. Interestingly, the quantum yields were found to be rather low, especially in nonpolar solvents, decreasing in the order of MACAIN > ACAIN > CACAIN. ACAIN reacts rapidly and quantitatively with simple thiols in a thiol-ene type click reaction. Using propanethiol, thiophenol, and cysteine as thiols complete

disappearance of the acryl double bond was observed in 5 min at room temperature in DMSO without any catalyst using the thiols in a molar excess (Fig. 8.). The hydrothiolation reaction was accompanied by a significant increase in fluorescence intensity depending on the solvent used.

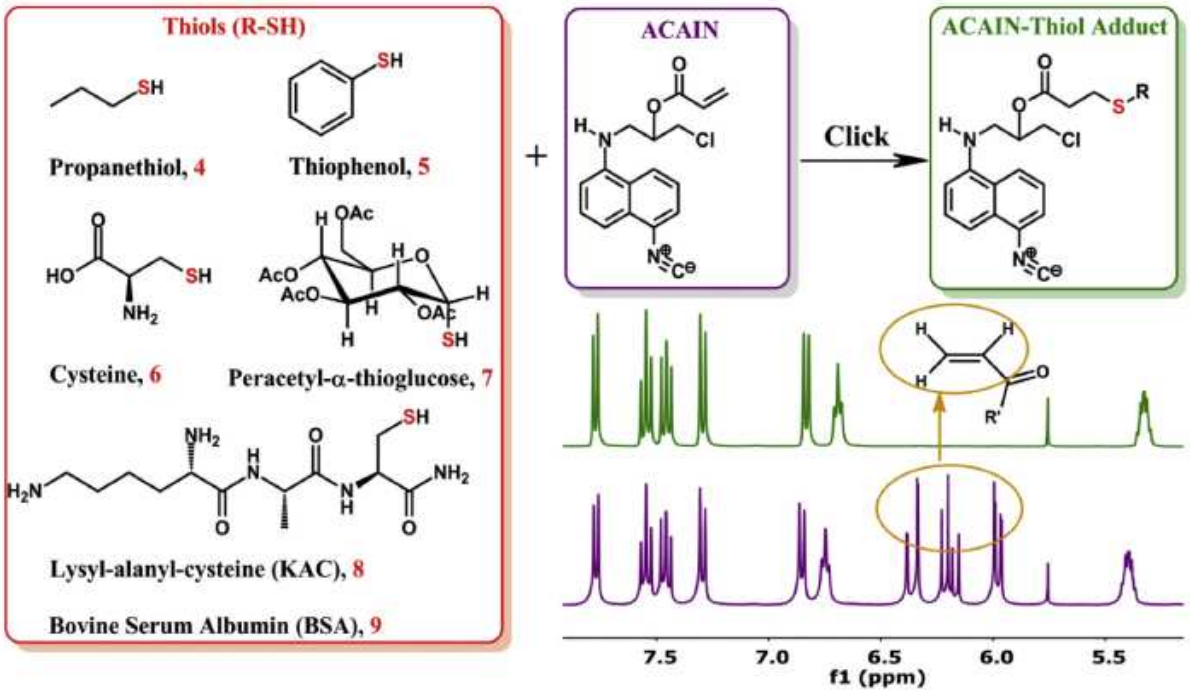

Figure 8. The thiol-ene click reaction of ACAIN with different thiols. The inset NMR spectra show the aromatic and olefin region of ACAIN (purple, bottom) and the ACAIN-propanethiol reaction mixture after 5 min (green, top).

The brightening of the addition product is due to the saturation of the acrylic group and can be applied in the fluorometric monitoring of the hydrothiolation reactions. In the case of MACAIN no such reaction could be observed, while CACAIN proved to react 100 times faster in DMSO than ACAIN. Unfortunately, the improved reactivity owing to the chloroacryl moiety drastically reduces the hydrolytic stability of CACAIN, whereas ACAIN is stable under the same conditions. The biolabeling properties of ACAIN were investigated in detail by both fluorometry and ESI mass spectrometry using cysteine, lysyl-alanyl-cysteine (KAC) and BSA as a model protein. The fluorescence intensity *versus* time curves for the reaction of ACAIN with cysteine, KAC and BSA at different pH are shown in Fig. 9.

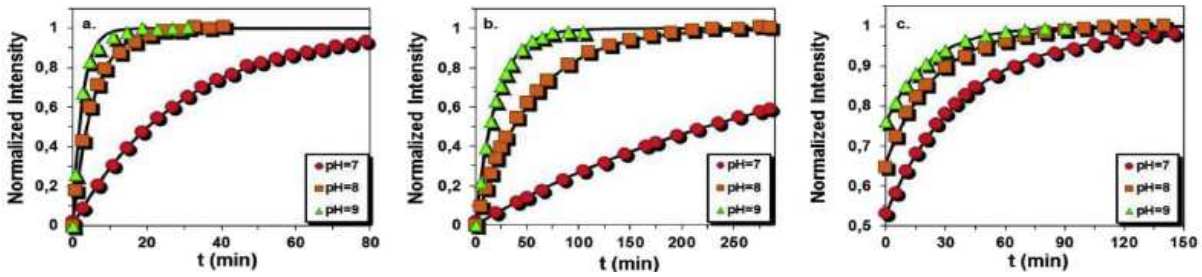

Figure 9. The fluorescence intensity *versus* time curves for the reaction of ACAIN with cysteine (a) (λ_{em}=505 nm), KAC (b) (λ_{em}=505 nm) and BSA (c) (λ_{em}=460 nm). Experimental conditions: $[cysteine]_o$ = $[KAC]_o$ = $[BSA]_o$ = 50 μM, $[ACAIN]_o$ = 6.3 μM, T = 20 ^oC. The relative intensities are given as $(I-I_o)/(I_\infty- I_o)$, where I is the intensity at time t, I_o the initial and I_∞ the final fluorescence intensity.

As seen in Fig. 9 the fluorescence intensities increase with time until plateau values have been reached indicating the completion of the reaction, i.e., covalent binding of all ACAIN molecules to the target compounds through acryl-thiol reaction. Moreover, in the case of BSA as can be seen in Fig. 9 c., there are large increases in the fluorescence intensity at the very beginning of the reaction followed by much slower increases in the fluorescence intensities. The initial, very sharp and large increase in the fluorescence intensities, which occur instantly upon adding of BSA to the ACAIN solution, can be ascribed to the fast non-covalent binding of ACAIN molecules. From the kinetics curves presented in Fig. 9. the values of the pK_a of the thiol groups in these coumpounds were also determined, which were found to be in good agreement with those reported in the literature.

In the following, the selectivity of the labeling was tested using KAC. Investigating the reaction by ESI-MS/MS method no fragment ions could be found where ACAIN labelled the lysine NH_2 group, only the hydrothiolation reaction with the cysteine SH group was observed. However, when labeling BSA two series of labelled products could be identified in the ESI-MS spectrum belonging to the molecules containing one and two ACAIN molecules attached covalently. Additional attachment of ACAIN to BSA most probably occurs on the only activated lysine unit of BSA in a hydrophobic pocket as was described earlier for Acrylodan, a well-known biolabeling dye. The optical properties of ACAIN and its SH adducts were described by high level quantum chemical calculations. The optimized structures revealed the formation of an intramolecular hydrogen bond between the NH and C=O moieties. This intramolecular H-bond gives rise to a dark nonfluorescent S_1 state due to a charge transfer from the amino-isocyanonaphthalene ring to the acryl group of ACAIN which is also close to a triplet state from which the molecule can return to the ground state through nonradiative decay. When the double bond is saturated by the SH addition the internal conversion pathway

leading to nonradiative decay ceases to exist resulting in the increase of the fluorescence quantum yields of the thiolated products. The brightening is more pronounced (15-19 fold) in nonpolar solvents where the majority of the starting ACAIN molecules is locked in the internal H-bonding position and only moderate (1.5-2 fold) in polar solvents where the solvent can break up the H-bond. Based on our DFT calculations the structure of the spacer has little effect on the electronic transitions as long as the internal H-bond can form. The situation significantly changes when the modification is carried out on the acrylic part. When the acryl group is replaced by a methacryl group i.e. an electron-donating group is introduced on the double bond the calculations showed an increased singlet-triplet gap which means a less probable internal conversion. Indeed, after preparing and investigating the properties of MACAIN a good correlation between the experimental quantum yield and the calculated singlet-triplet energy difference was found. Also, if an electron withdrawing chlorine atom is used instead of the methyl group calculations show the tightening of the singlet-triplet gap, which could be applied in the construction of molecular switches based on ACAIN.

VI. Acrylated isocyanonaphthalenes for staining living plant cell

We demonstrated that the isocyanonaphtalene fluorophore derivatives 1-(2-acryloyloxy-3-chloro-prop-1-yl)-amino-5-isocyanonaphthalene (ACAIN) and (2-chloroacryloyloxy-3-chloroprop-1-yl)-amino-5-isocyanonaphthalene (CACAIN) are able to bind cysteine-rich proteins with hydrophobic motifs. In this study, we focused our work on the practical application of these fluorophores for living plant cell staining. When living Col-0 plants were stained with ACAIN and visualized with a conventional fluorescence microscope, specialized shoot epidermal cells (trichomes and guard cells) as well as hypocotyl cortex cells showed endomembrane labeling. Thus, labeling pattern raised the possibility of ACAIN binding to vacuolar membranes (Fig. 10a–d). Therefore, in the next step, we labeled whole Arabidopsis seedlings expressing GFP-TIP2;1, (green fluorescent protein) known for the characteristic tonoplast GFP signal. ACAIN and GFP signals showed a perfect co-localization in hypocotyls (Fig. 10e).

Labeling of Col-0 and GFP-TIP2;1 seedlings showed the presence of large vacuoles as well as smaller tonoplast-coated vesicles in hypocotyl epidermal and cortex cells (Fig. 10e, f). preferentially label tonoplasts in living *Arabidopsis* and tobacco (*Nicotiana tabacum* SR1) cells. ACAIN-labeled membranes co-localized with the GFP signal in plants expressing GFP-δ-TIP (TIP2;1) (a tonoplast aquaporin) fusion protein. ACAIN could label tonoplasts in

hypocotyl cells of tobacco (*N. tabacum* SR1) as well, in a similar manner to Arabidopsis (Fig. 10f, g). The fluorophore ACAIN preserved cell viability and vacuolar dynamics, thus it proved to be suitable for live cell imaging. For differentiated or meristematic cells of Arabidopsis roots, labeling was weaker and more diffuse, but this was true for the GFP signal in GFP-TIP2;1 roots as well (Fig. 10h).

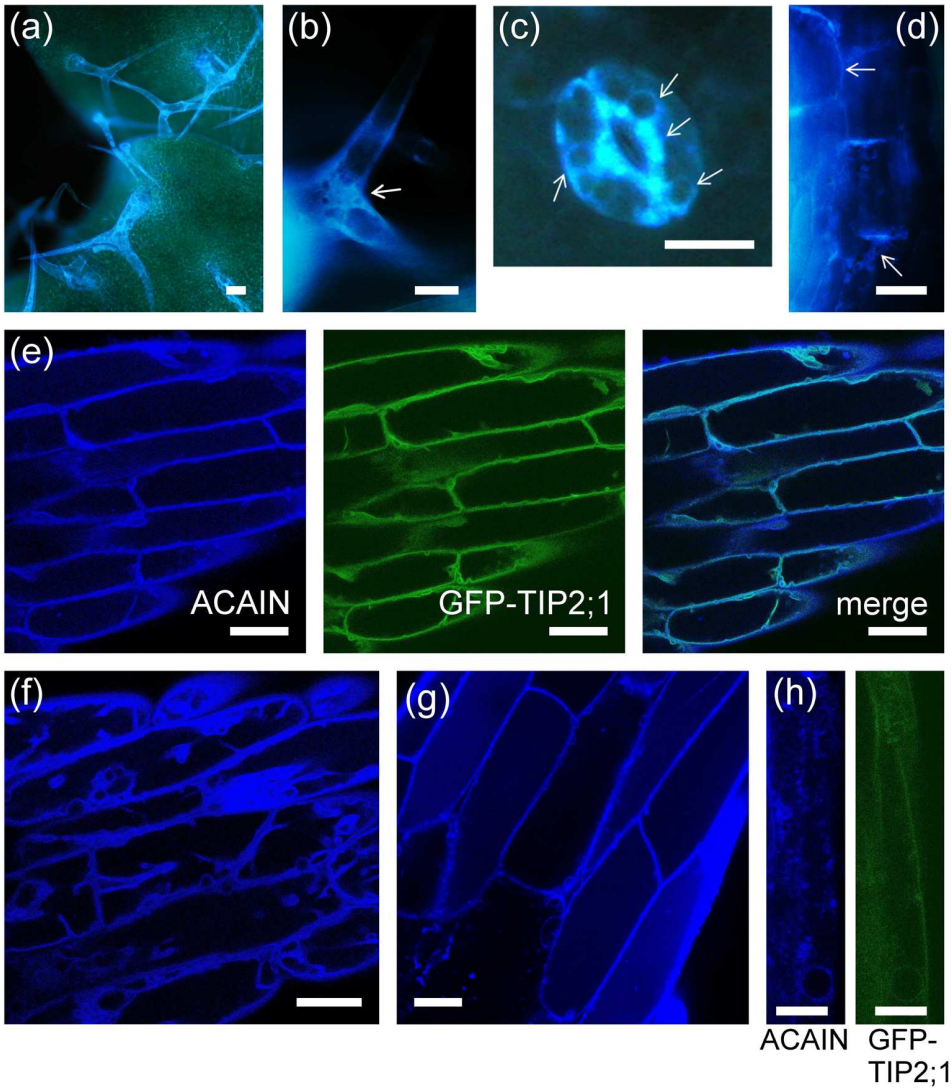

Figure 10. ACAIN labels preferentially tonoplasts in living plant cells. All images were taken from *Arabidopsis* seedlings, except (g) that was of hypocotyls from *N. tabacum* SR1 seedlings. Images of (a)–(d) are of conventional fluorescence microscopy with arrows indicating the labeling of membrane structures. (e)–(h) are CLSM images. ACAIN labeling (a) of trichomes, (b) detail of trichome labeling, (c) of hypocotyl guard cells, and (d) of hypocotyl cortex cells from Col-0 plants. Conventional fluorescence microscope images show the probability of endomembrane labeling. e ACAIN labeling of a Triton X-100 permeabilized hypocotyl segment of Arabidopsis Col-0 plants containing GFP-tagged δ-TIP (TIP2;1) protein. ACAIN label colocalizes with TIP2;1. f, g ACAIN labeling of hypocotyl cells not permeabilized with Triton X-100 from *Arabidopsis* Col-0 (f) and N. tabacum SR1 (g). h ACAIN labeling of Triton X-100 permeabilized differentiated cells of root from Arabidopsis plants containing GFP tagged δ-TIP (TIP2;1) protein. Both ACAIN and GFP signals are diffuse, showing multiple tonoplast-coated vesicles. Scale bars: 30 μm

Furthermore, ACAIN preserved the dynamics of vacuolar structures. tip2;1 and triple tip1;1-tip1;2-tip2;1 knockout mutants showed weaker ACAIN signal in tonoplasts. The ACAIN is also suitable for the labeling and detection of specific (cysteine-rich, hydrophobic) proteins from crude cell protein extracts following SDS-PAGE and TIP mutants show altered labeling patterns; however, it appears that ACAIN labels a large variety of tonoplast proteins.

We extended our investigations to the possible use of ACAIN/CACAIN for the study of stress-induced changes of vacuolar organization. We used microcystin-LR (MCY-LR) for this purpose. This toxin is widely used as a tool for the regulation of structural organization and dynamics of subcellular compartments. According to these experiments, we obsereved that ACAIN/CACAIN could be used for the detection of altered vacuolar organization induced by the heptapeptide natural toxin microcystin-LR (MCY-LR), a potent inhibitor of both type 1 and 2A protein phosphatases and a ROS inducer (Fig. 11a-k.).

As revealed both in plants with GFP-TIP2;1 fusions and in wild-type (Columbia) plants labeled with ACAIN/CACAIN, MCY-LR induces the formation of small vesicles, concomitantly with the absence of the large vegetative vacuoles characteristic for differentiated cells. TEM studies of MCY-LR-treated Arabidopsis cells proved the presence of multimembrane vesicles, with characteristics of lytic vacuoles or autophagosomes. Moreover, MCY-LR is a stronger inducer of small vesicle formation than okadaic acid (which inhibits preferentially PP2A) and tautomycin (which inhibits preferentially PP1).

Summarizing our results obtained on staining with the fluorophores ACAIN and CACAIN. They can be of universal use for the preferential labeling of tonoplasts in living plant cells and the study of tonoplast dynamics. Therefore, they may be good alternatives to the use of tonoplast-specific GFP-fusion proteins widely used for this purpose. These fluorochromes are suitable for the detection of stress-related changes of vacuolar organization as revealed by treatments with protein phosphatase inhibitors. In addition, even though ACAIN labeling is not restricted to a single protein with hydrophobic motifs, it is suitable for the detection and possible further identification of proteins with cysteine-rich hydrophobic motifs, among them tonoplast-specific proteins following SDS-PAGE. In addition, ACAIN and CACAIN emerge as useful novel tools to study plant vacuole biogenesis and programmed cell death.

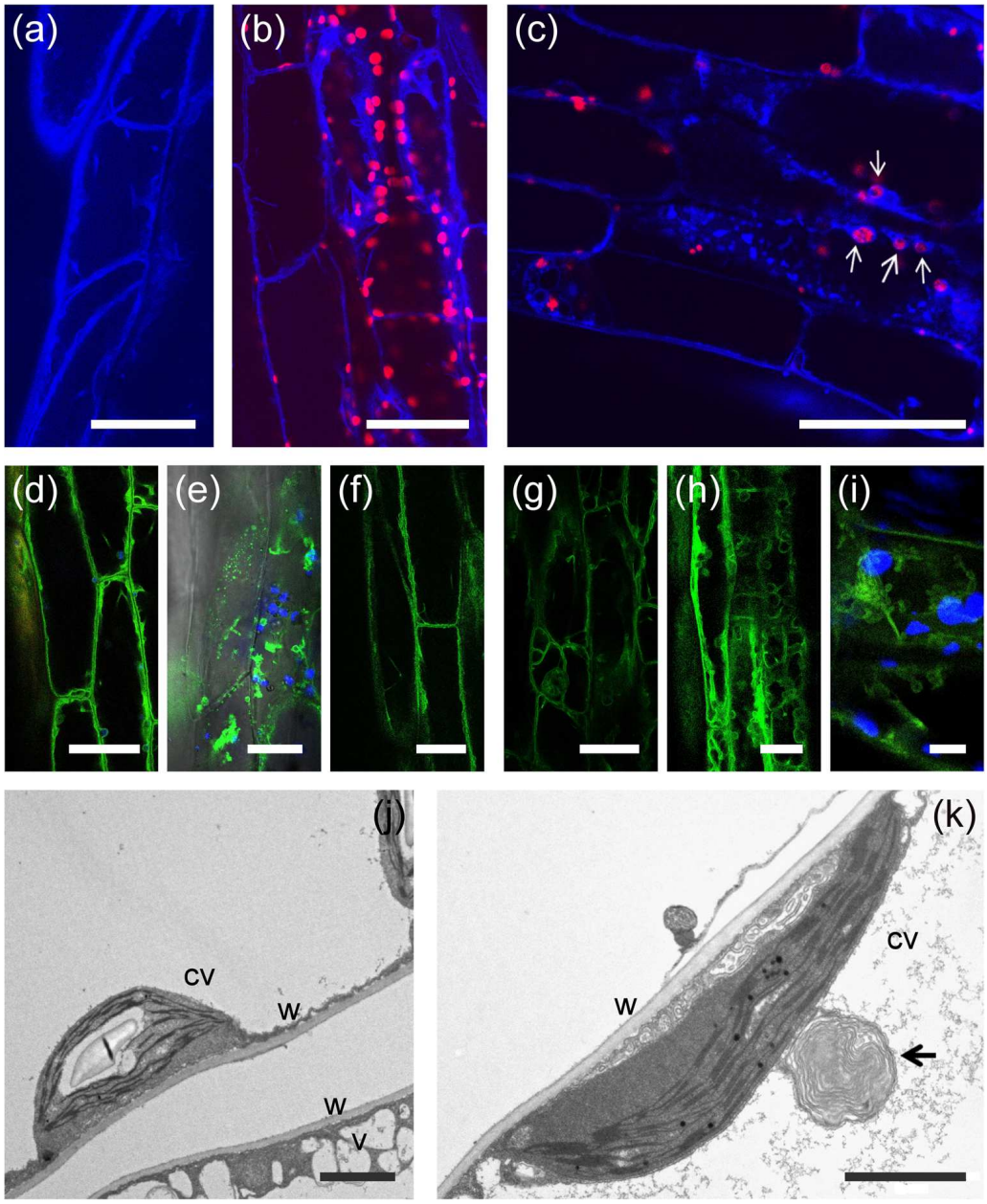

Figure 11. CACAIN labeling in Col-0 (a–c) and analysis of GFP-TIP2;1 (d–i) hypocotyls reveal changes of vacuolar organization in hypocotyl cells treated with protein phosphatase inhibitors. a Control, ACAIN labeling, normal vacuolar system; b control, CACAIN labeling, tonoplasts (blue) and chloroplast autofluorescence (red); c treatment with 5 µM microcystin-LR (MCY-LR) for 24 h, CACAIN labeling. Disorganization of the vacuolar system and capturing of chloroplasts by tonoplast-coated vesicles (arrows). d Control, normal vacuolar system; e 1 µM MCY-LR, 4 h treatment showing numerous tonoplast-coated vesicles; f 1 µM okadaic acid (OA), 24 h—no visible changes in the vacuolar system. g Control in the presence of MS medium with 0.1% DMSO (tautomycin, Tm, treatments were made with stocks of the inhibitor diluted in DMSO). Treatments with 1 µM Tm for 9 h (h) and 24 h (i) show disorganization of the vacuolar system. i. j TEM image of a control hypocotyl cell showing chloroplasts and normal endomembrane system; k TEM image of a hypocotyl cell treated with 2 µM MCY-LR for 3 days, showing a multimembrane vesicle (arrow). Legends for (j), (k): cv, central vacuole; v, vesicle belonging to the vacuolar system; w, cell wall. Scale bars: 30 µm (a–h), 10 µm (i), 2 µm (j, k)

VII. Application of solvatochromic isocyanonaphthalene dyes in silver(I) detection and backgroundreduction in biolabelling

In this research, we studied the complex formation of solvatochromic 1-amino-5-isocyanonaphthalene (ICAN) derivatives (Scheme 2.) with Ag(I) ions.

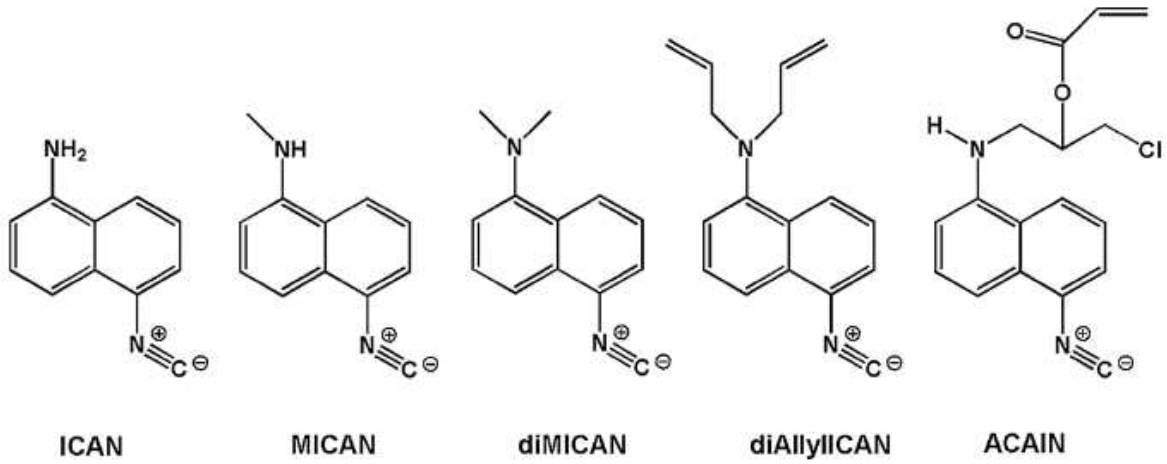

Scheme 2. The structure and name of the ligands used for complexation of Ag(I)-ions.

UV–vis and steady-state fluorescence spectroscopic results revealed the exclusive presence of 1:1 complexesin solutions in concentrations below 10 mM. We observed that by increasing the concentration, independently of the ratio of the Ag(I) and ligand theformation of a solid yellow precipitate was observed, which was identified as the 1:2 AgL_2 complex. The 1:2 complex can be redissolved in DMSO, where based on ^{1}H-NMR it is the only species in solution. The 1:1 complex, however, cannot be prepared in a solid form and the 1:2 complex was not detected in other solvents. The formation of the 1:1 complex in organic solvents is accompanied by a significant batochromic shift in both the absorption and the emission spectra ($\Delta\lambda_{abs}$= 19–32 nm $\Delta\lambda_{em}$= 30–59 nm) (Fig. 12 and Fig. 13). The red shifts were found to be largely solvent dependent: in water they were negligible, whereas the largest $\Delta\lambda_{em}$ values were measured in moderately polar solvents such as chloroform and dioxane. In contrast, $\Delta\lambda_{em}$ did not show a significant variation with different counterions (TFA, BF_4^-, and ClO_4^-) and the N-substituent of the ligand. For most of the ICAN ligands the quantum yield of the complex was lower than that of the free ligand, and the opposite is valid in the case of ACAIN.

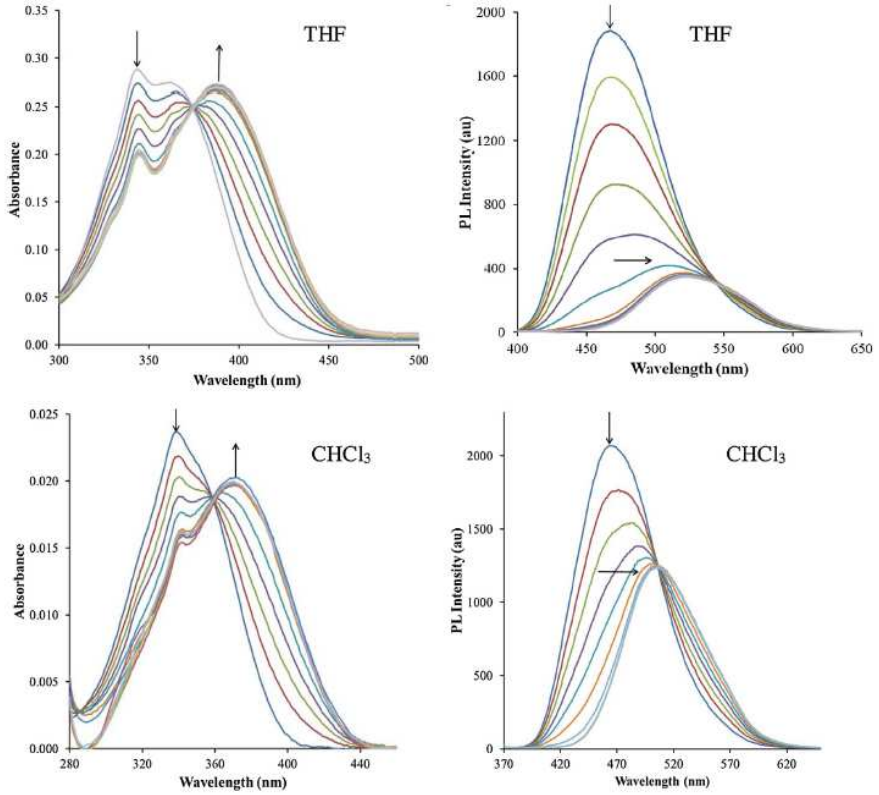

Figure 12. The absorption and emission spectra of ICAN recorded in THF and $CHCl_3$. The highest intensity peak indicated with the downward arrow always belongs to pure ICAN (c_{ICAN}= 5 × 10^{-5} M). Each additional line represents the addition of 34.4 nanomole of AgTFA.

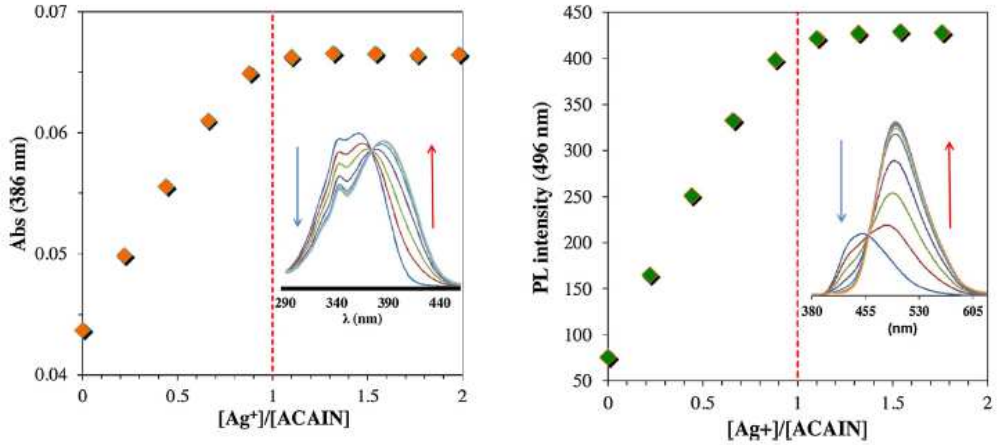

Figure 13. The change of absorbance and fluorescence as a function of metal (Ag^+) and Ligand (ACAIN) concentration ratio. The insets show the raw spectral changes during thetitration experiments. (T = 20 ˚C, [ACAIN] = 1.04 × 10^{-5} M).

These fluorescence switch-off and -on phenomena can be favorably used in practical applications. The equilibrium constants were found to be K = 10^6–10^7 M^{-1} in dioxane and ~10^4 M^{-1} in acetonitrile, where competitive complexation of Ag(I) with the solvent is present. Time resolved fluorescence measurements showed that the fluorescence decay rates of the

complexes were nearly equal ($k \sim 7 \times 10^7\ s^{-1}$) but also revealed the increased rate of nonradiative decay processes in 1:1 complexes compared to the free ligands. However, the radiative decay rate increased after the complexation of ACAIN with Ag(I), which was caused by the termination of an internal quenching pathway in the uncomplexed ligand. The structure and optical properties of the complexes were explained by high-level quantum chemical calculations. DFT calculations revealed a linear orientation of the 1:1 complex, where in the lowest energy isomer the silver(I) ion coordinates to the isocyano moiety. Based on the M06 functional the calculated wavelength shifts match the experimental values. Fluorescence quenching in the case of ICAN may be accounted for by the possible formation of π-stacked dimers in an anti-periplanar orientation, where it is possible that a charge transfer between the rings quenches the emission. 2:2 type complexes were also investigated and their presence were excluded in solution since either they broke into two 1:1 fragments or gave high energies during optimization. The practical applications of the 1:1 complexes were demonstrated by two examples. ACAIN in dioxane:water 9:1 mixture proved to be a highly selective analytical reagent for the quantitative determination of aqueous Ag(I)-ions (Fig. 14.). The fluorescene swhitch-off in the 1:1 AgL complexes of ICAN can be advantageously applied in biolabeling processes due to thereduced background flluorescene (Fig. 15.). It was found that the complex disintegrates after binding to proteins, while it is higly stable inaqueous solution. In addition, MICAN:Ag 1:1 complex was shown to enhance the contrast during the staining of HACaT cells while no observable difference between the stainig ability of the free MICAN and its Ag complex could be observed. The details and brightness of the stained cells are the same.

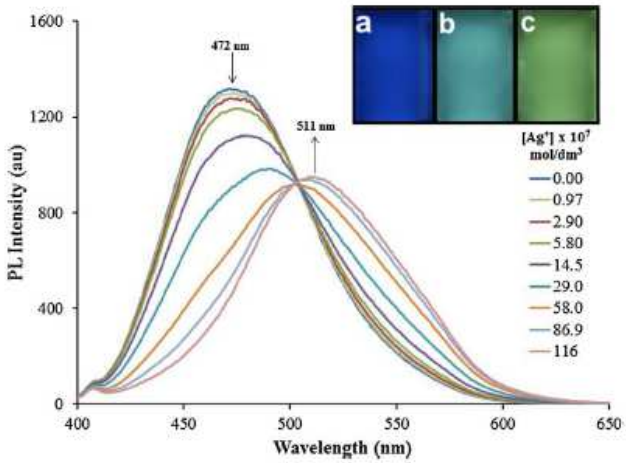

Figure 14. Spectral changes upon the addition of different amounts of $AgNO_3$ to the solution of ACAIN in dioxane:water 9:1 (v/v). The inset picture shows ACAIN inpure dioxane (a), in dioxane:water 9:1 (v/v) (b) and after the addition of 2 molar equivalent Ag^+ to solution b (c) ([ACAIN] = 4.69×10^{-6} M, T = 20 ˚C, λ_{ex}= 365 nm).

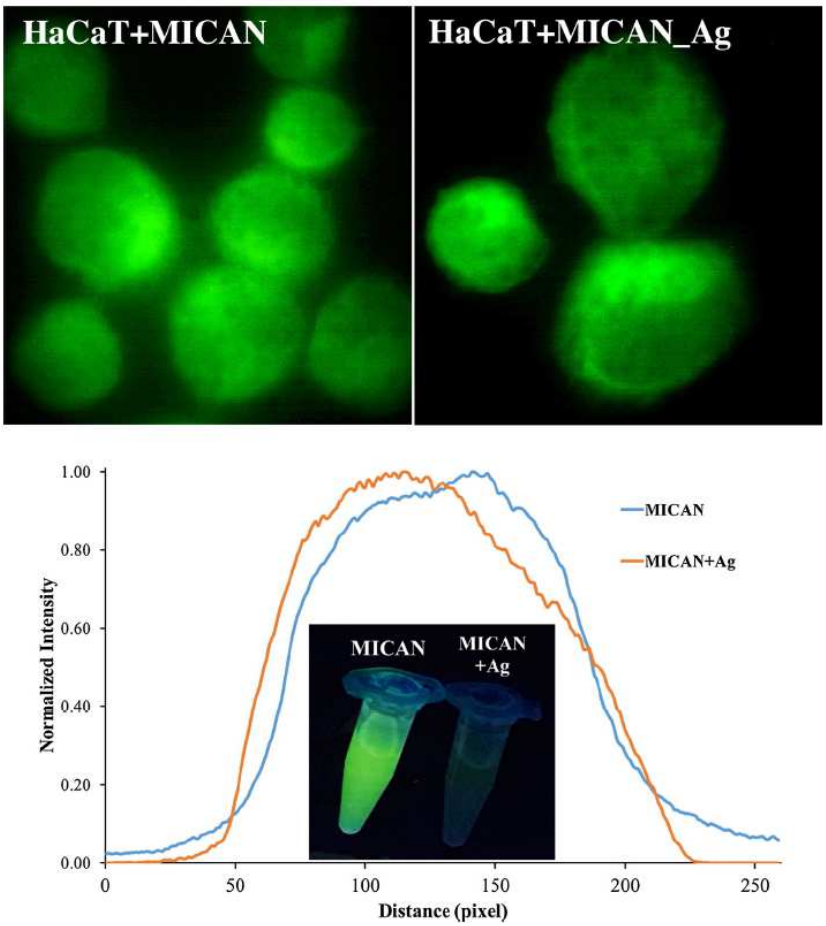

Figure 15. Fixated HaCaT cells stained with aqueous MICAN and MICAN:Ag 1:1 complex. The bottom plot shows the intensity-distance distribution for two HaCaT cells selected from the original of the upper images. The inset picture shows the starting aqueous stains under UV irradiation (λ_{ex}= 365 nm, [MICAN] = 22.0 μM).

VIII. Influence of gold nanoparticles on the fluorescence property of ACAIN

The fluorescence properties of organic molecules can be changed (enhanced or decreased) in the presence of metal nanoparticles. The presence of electromagnetic, plasmon field emitted by an excited metal nanoparticle can enhance the fluorescence or at the same time it can decrease if the fluoresecent molecule is directly connected to the metal surface because of the resonant transfer of excitation energy to the metal or due to the dissociation of excitons at the interface. Our goal was to combine ACAIN with the Au NP containing polymer matrix, which potentionally can be important compund for sensor applications, i.e., to enhance the fluorescence property of ACAIN by incorporating it into to a copolymer, so that it could be used as a starting material for solid state sensors. ACAIN were copolymerized with diurethane dimethacrylate (UDMA) and isodecyl acrylate (IDA) using 2,2-dimethoxy-2-phenylacetophenone (photo)initiator in a photopolymerization process in the presence of dodecanethiol-functionalized gold and SiO_2 nanoparticles (Fig. 16).

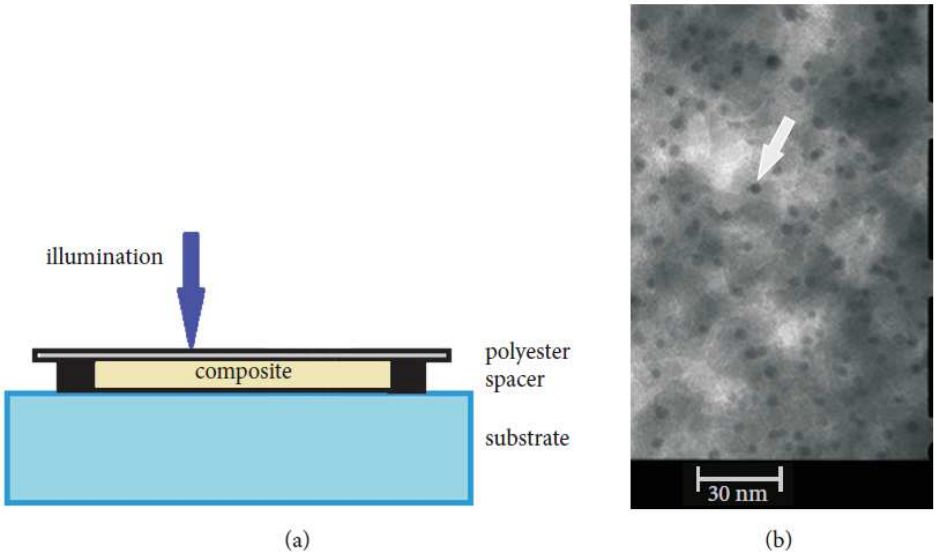

Figure 16. (a) Scheme of sample preparation. The polyester film is removed after polymerization. (b) TEM picture of AuNPs (the white arrow shows one of them).

The photoluminescence spectra of the composites prepared are presented in Fig. 17. It was found that the pure polymer matrix and the copolymer with Au and SiO_2 NPs were not luminescent, while introduction of ACAIN stimulated a strong luminescence signal. The last spectrum has wide asymmetrical band shapes with small maxima features at 460 and 490 nm for the ACAIN copolymer composite without and with SiO_2 nanoparticles, respectively. These spectra have similar shapes which is characteristic for naphthalene derivatives. However, the maxima are essentially shifted to the red spectral range, which can be explained by the presence of the N≡C group in the ACAIN.

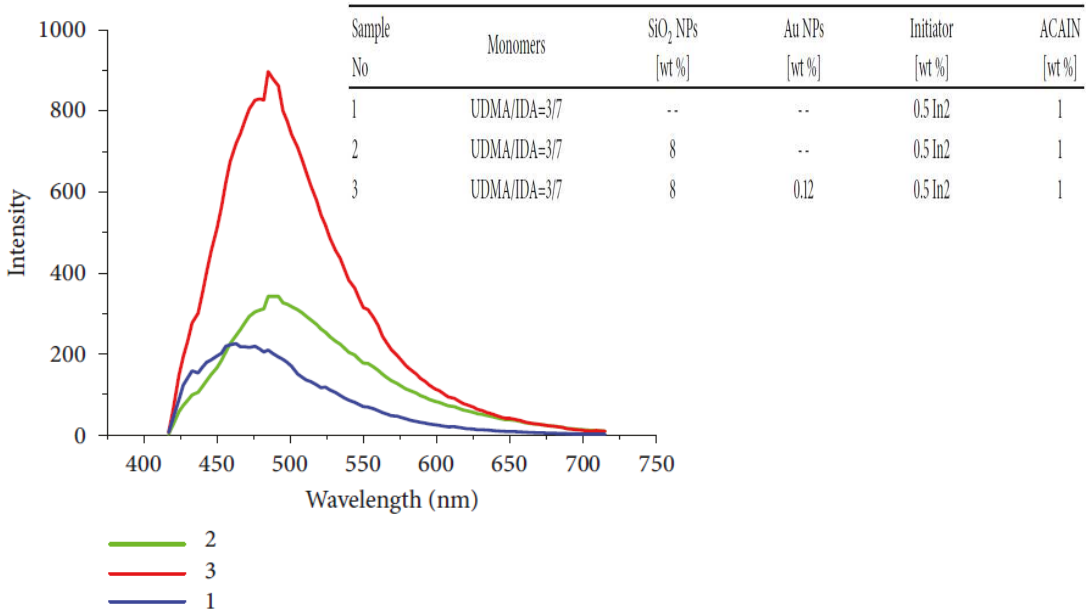

Sample No	Monomers	SiO_2 NPs [wt %]	Au NPs [wt %]	Initiator [wt %]	ACAIN [wt %]
1	UDMA/IDA=3/7	--	--	0.5 In2	1
2	UDMA/IDA=3/7	8	--	0.5 In2	1
3	UDMA/IDA=3/7	8	0.12	0.5 In2	1

Figure 17. Fluorescence spectra of the ACAIN-containing polymer films, compositions 1, 2, and 3.

It was also observed that introduction of SiO_2 nanoparticles to the UDMA/IDA/ACAIN copolymere increased the fluorescence intensity by 1.5 times, and the addition of Au NPs/SiO_2 results in a 4.5-time increase in the intensity (Fig. 17.). In addition to the effect of SiO_2 NPs and the essential role of Au NPs can be attributed to the generation of plasmon fields, which are localized near the Au NPs, causing an efficient interaction with the fluorescent molecules.

IX. Effect of the substitution position on the electronic and solvatochromic properties of ICAN)s

We also performed a detailed study on the electronic, fluorescent and solvatochromic properties of 1,4-isocyanoaminonaphthalene (1,4-ICAN) and 2,6-isocyanoaminonaphthalene (2,6-ICAN) isomers and compared them with those of 1,5-ICAN. In these isocyanoaminonaphthalene derivatives, the isocyano and the amine group served as the donor and acceptor moieties, respectively. It was found that the positions of the donor and the acceptor groups in these naphthalene derivatives greatly influence the fluorescence properties (Fig. 18.).

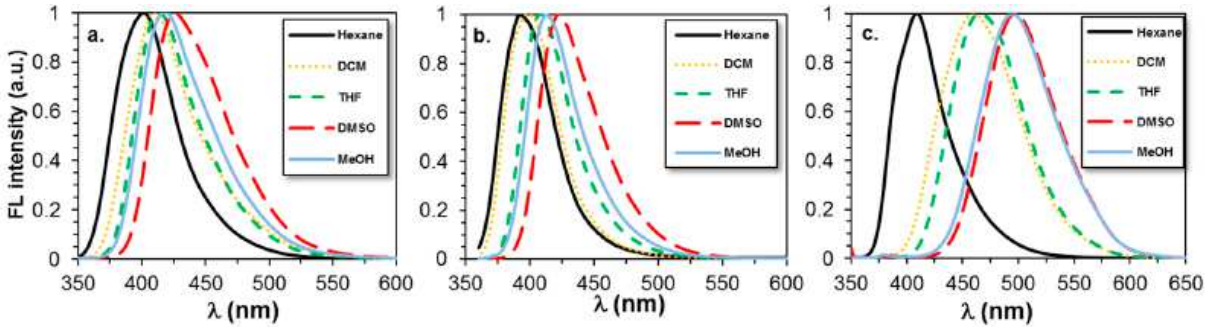

Figure 18. Normalized fluorescence emission spectra of the 1,4-ICAN (a), 2,6-ICAN (b), and 1,5-ICAN (c) isomers recorded in different solvents.

According to Fig. 18., the fluorescence emission spectra of both 1,4-ICAN and 2,6-ICAN in various solvents show unstructured, single bands, similar to those of 1,5-ICAN [15], revealing positive solvatochromic shifts upon increasing the solvent polarity from n-hexane to DMSO. In addition, the same is valid for the fluorescence emission bandwidth at half maximum ($\Delta\nu_{1/2}$), which may be indicative of the extent of intramolecular charge transfer (ICT) upon excitation.

In order to quantify the solvatochromic effect induced by the solvents of different polarity, the fluorescence emission maxima (ν_{Em}) were plotted as a function of the empirical solvent polarity parameter $E_T(30)$ and the Lippert–Mataga (LM) plot, i.e., a plot for the Stokes shifts ($\Delta\nu_{SS}$) *versus* (Δf_{LM}) were constructed (Fig. 19).

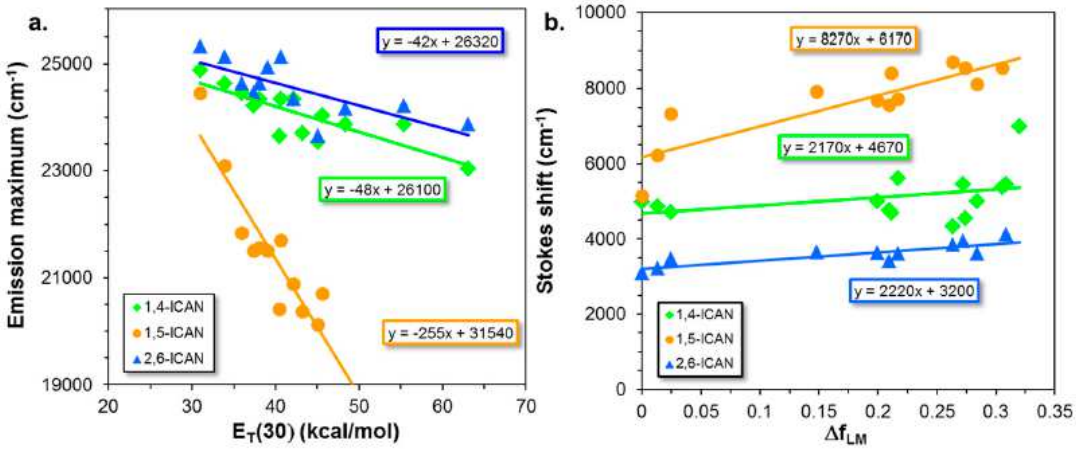

Figure 19. Variation of the fluorescence emission maximum with the empirical solvent polarity parameter $E_T(30)$ (a), and the Lippert–Mataga (LM) (b), plots for the 1,4-ICAN, 1,5-ICAN, and the 2,6-ICAN isomers.

From the LM-plots (Fig. 19b.), the corresponding differences in the dipole moments of the excited and the ground states were determined, and good agreements with the DFT calculations were obtained (Table 1.).

Table 1. The Onsager-radius (a_o), dipole moment difference between the excited and the ground state ($(\mu_E-\mu_G)_{DFT}$) calculated by DFT, and the dipole moment differences in the excited and ground state ($(\mu_E-\mu_G)_{LM}$) determined by the Lippert-Mataga equation.

	a_o (pm)	$(\mu_E-\mu_G)_{DFT}$ (D)	$(\mu_E-\mu_G)_{LM}$ (D)
1,5-ICAN	305	4.8	4.9
1,4-ICAN	278	0.7	2.2
2,6-ICAN	388	3.5	3.6

Furthermore, the time-resolved fluorescence emission experiments revealed that (i) emissions take place from the solvent-relaxed state. (ii) both k_r and k_{nr} showed a minimum value as a function of the solvent polarity parameter $E_T(30)$ for the 1,5-ICAN and 1,4-ICAN isomers in DMSO, but for the 2,6-ICAN isomer, k_r was found to be nearly constant in the range of the solvent polarity parameter investigated (Fig. 20).

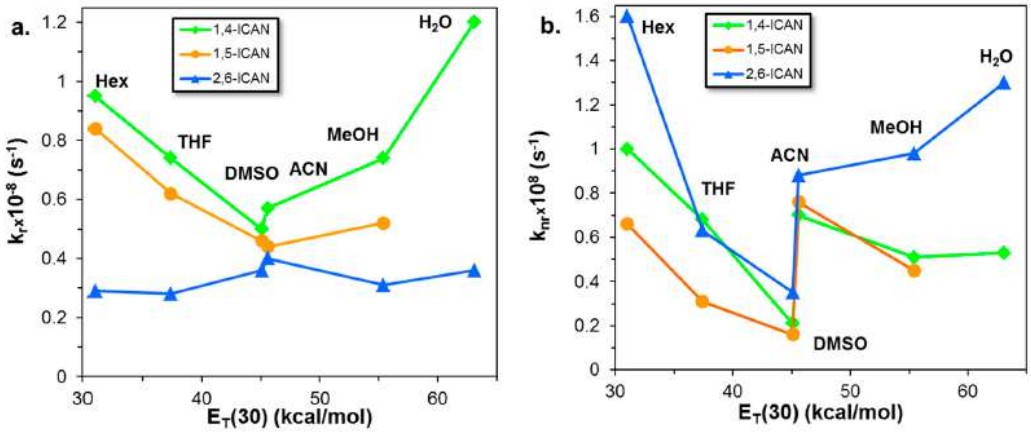

Figure 20. The variation of the radiative decay rate (k_r) (a) and the non-radiative decay rate (k_{nr}) (b) the with the empirical solvent polarity parameter $E_T(30)$.

X. Amino-isocyanoacridines: novel, tunable solvatochromic fluorophores as physiological pH probes

In a next series of experiments, the aromatic moiety was modified to obtain 3-amino-6-isocyanoacridine (ICAAc), and with further reactions of ICAAc with CH_3I we were able to synthesize 3-N-methylamino-6-isocyanoacridine (monoMICAAc) and 3-N,N-dimethylamino-6-isocyanoacridine (diMICAAc) derivatives (Scheme 3.)

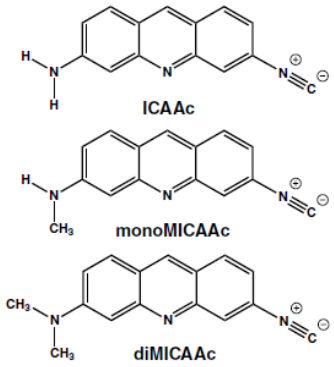

Scheme 3. The structures and names of the dyes used in this study. 3-amino-6-isocyanoacridine (ICAAc), 3-N-methylamino-6-isocyanoacridine (monoMICAAc), 3-N,N-dimethylamino-6-isocyanoacridine (diMICAAc).

These ICAAcs derivatives proved to be a multifunctional acridine orange (AO) type dye family with a number of additional favorable properties such as enhanced solvatochromic emission range and low quantum yields (Φ_F = 2.9–0.4%) in water (Fig. 21.)

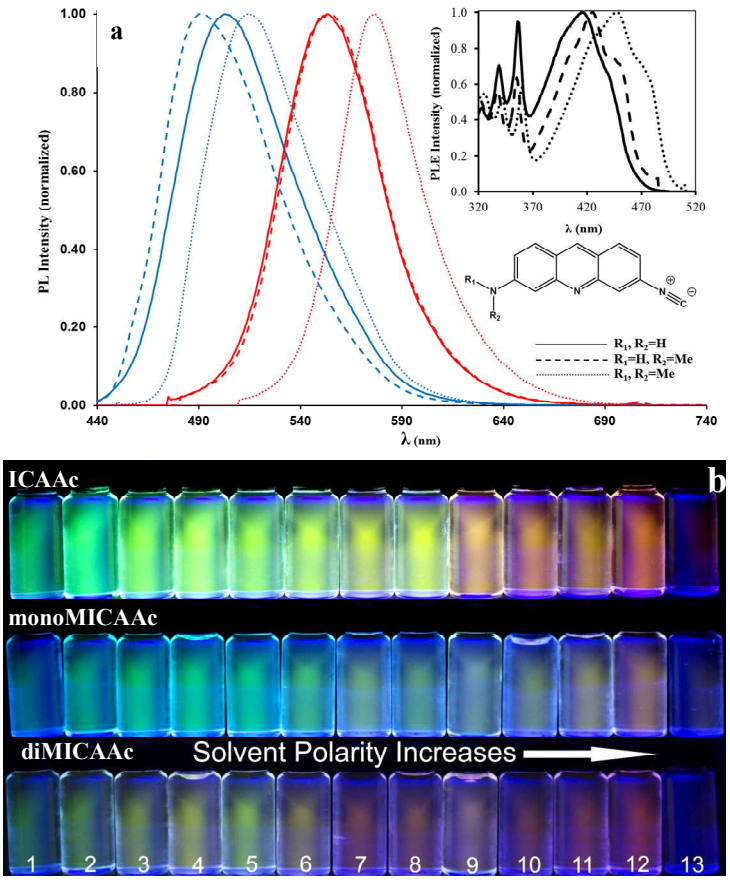

Figure 21. (**a**) The normalized emission spectra of the isocyanoacridine dyes recorded in hexane (blue) and water (red). The inset shows the excitation spectra recorded only in hexane. (**b**) Demonstration of the fluorescence properties of the **ICAAc** derivatives in different solvents (λ_{ex}=365 nm). Solvents from left to the right are hexane (1), toluene (2), 1,4-dioxane (3), CH_2Cl_2 (4), $CHCl_3$ (5), THF (6), MeCN (7), acetone (8), pyridine (9), methanol (10), DMF (11), DMSO (12), water (13).

Furthermore, it is known that acridine based dyes such as acridine orange AO can be present in different forms in aqueous media. To characterize the acid-base properties of our **ICAAc** derivatives UV-vis and steady-state fluorescence measurements were carried out in the pH range of 2-12 using Britton–Robinson "universal" buffer (BRB) (Fig. 22.)

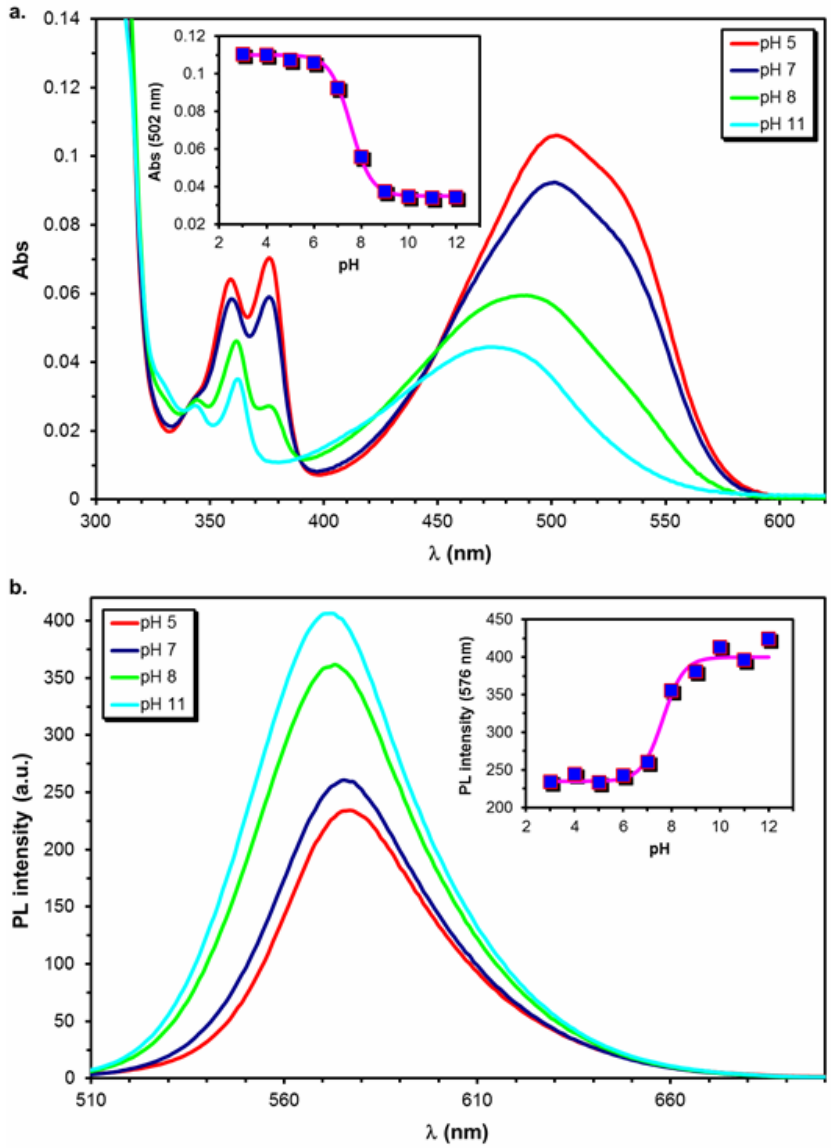

Figure 22. Demonstration of the changes in the UV-vis absorption (**a**) and emission (**b**) spectrum of **diMICAAc** in BRB at different pH. The insets show Eq. 1 fitted on the experimental absorbance or PL intensity data. (T=20 ºC. ([dye] = 4.58×10^{-5} M), V=3.00 cm^3).

We found that the pK_a value of **diMICAAc** is 7.5, which falls in the physiological pH range, thus making it a possible candidate for a fluorescent biosensor (Fig. 23.). In addition, ICAAcs can be applied as stable pH-probes with great precision (2–3% error) in the physiological pH range of 6–8 using UV-vis and fluorescence detection.

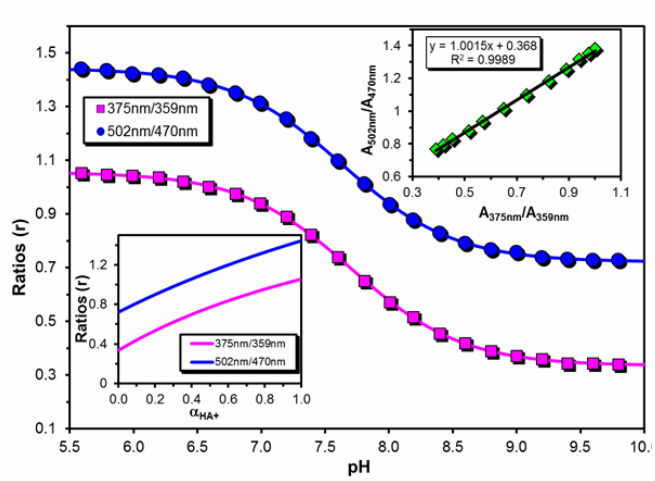

Figure 23. UV-vis titration curves of **diMICAAc** in BRB buffer at different pHs. The lines were fitted using Eq. 2. The bottom left inset shows the absorbance ratios as a function of the molar fraction of the protonated form α_{HA+}. The top right inset shows the correlation between the absorbance ratios calculated at the ICT and acridine like absorption wavelengths. (T=20 ºC, [dye] = 1.14×10^{-5} M, V=3.00 cm^3).

The optical behavior of ICAAcs could be fine-tuned by complexation with Ag(I) ions, too (Fig. 24.).

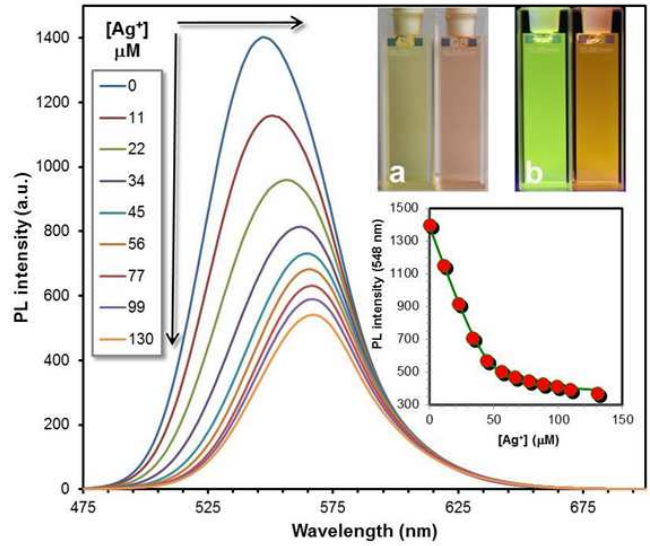

Figure 24. The change of fluorescence as a function of metal (Ag^+) concentration in the dioxane solution of **diMICAAc** (4.58×10^{-5} M). Picture (**a**) **diMICAAc** in dioxane (left) and in the presence of 130 μM Ag^+ (right) under visible light. Picture (**b**) the same compositions as in (**a**) illuminated by λ_{ex}=365 nm UV-light.

Steady-state fluorescence titration of diMICAAc in dioxane revealed a sharp decrease of PL intensity (to one-third of the original) with increasing silver(I) concentration as shown in Fig. 24. In addition, a 20 nm bathochromic shift of the emission maximum occurs from $\lambda_{em,max}$=548 nm to $\lambda_{em,max}$=568 nm, which manifests in a color change from greenish-yellow to

red in visible light and from neon green to orange when excited with λ_{ex}=365 nm UV light (Fig. 24. insets a and b respectively). The shape of the inset graph in Fig. 24 indicates the formation of a 1:1 complex, which was also detected under ESI-MS conditions.

The equilibrium constant of complexation was determined using non-linear regression analysis and was found to be K=(4.5±0.9)x10^5 M^{-1}. Moreover, this equilibrium constant is lower than those obtained for ICAN derivatives (K =10^6 M^{-1} and 10^7 M^{-1}) but it still indicates high binding affinity of silver(I) towards diMICAAc. The formation of a 1:1 complex is further backed by quantum chemical (DFT) calculations since the calculated PL spectrum agrees very well with the measured. DFT calculations also revealed that Ag^+ is attached to the isocyano moiety instead of the imino nitrogen in the ring (Fig. 24.).

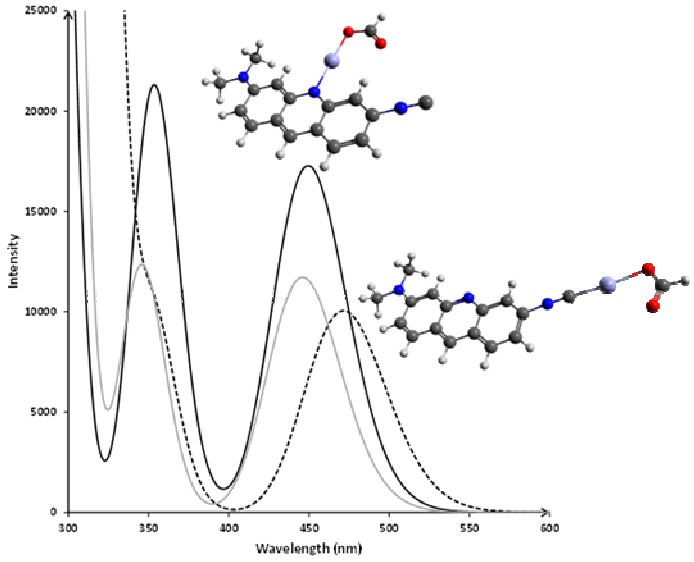

Figure 24. The calculated UV-vis absorption spectra of the two Ag:diMICAAc complexes together with the diMICAAc (grey line) The ground state Gibbs free energy difference between the two forms is only 0.9 kcal mol^{-1}.

24 hour MTT assays on HeLa cells revealed LD_{50} values of 7.27, 5.78, and 7.50 μM for **ICAAc**, **monoMICAAc** and **diMICAAc** dyes, respectively. We also demonstrated the applicability of **ICAAc**, **monoMICAAc**, and **diMICAAc** dyes for live cell imaging on HeLa cells at 0.3 μg/ml dye concentration. **diMICAAc** stained cells demonstrated the best-preserved morphology. According to our investigations **DiMICAAc** probably binds cell membranes, some unknown intracellular vesicular structures, probably the DNA slightly, and possible binds to some extent to the RNA. All three dyes are well-applicable with conventional epifluorescence imaging. Furthermore, at the blue excitation, diMICAAc is optimally suited as a whole-cell probe for both the conventional microscopic and the laser-

illumination studies, like flow- and imaging cytometric, or confocal laser-scanning microscopic examinations (Fig. 25.).

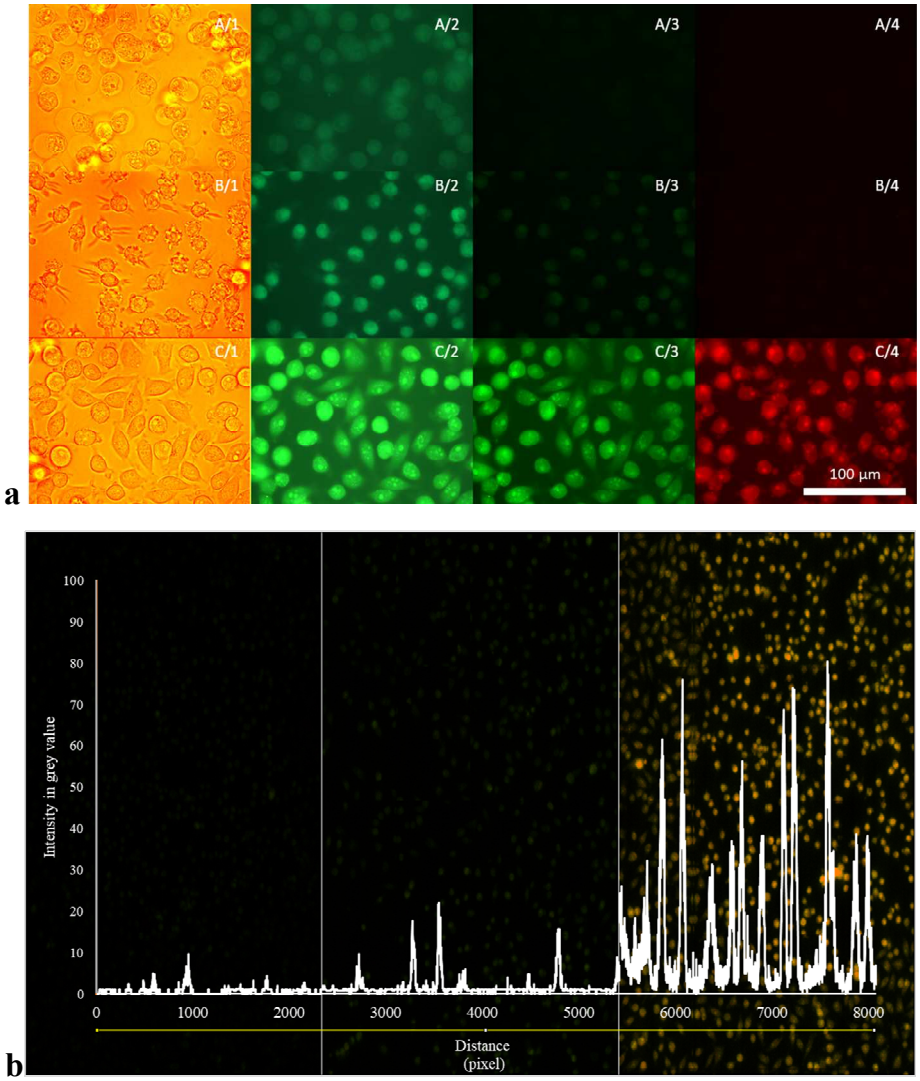

Figure 25. (**a**) Demonstration of the staining capacity of **ICAAc** derivatives for live cell imaging in HeLa cells. The following staining arrangement was applied: (A) **ICAAc**; (B) **monoMICAAc**; (C) **diMICAAc**. In column #1: bright field; in column #2: UV/blue fluorescence; in column #3: blue/green fluorescence; in column #4: green/red excitation/emission epifluorescence illumination was employed. (**b**) Quantitative comparison of cell staining capacity of the new dyes applying imaging cytometry. Mosaic scan images of vitally stained HeLa cells were made for the **ICAAc** (left panel), **monoMICAAc** (middle panel), and **diMICAAc** dyes (right panel) applying iCys laser-scanning cytometer with the same excitation and detection settings. 488 nm laser illumination and 530±15 nm emission were used to make images. The cell staining intensity profile was plotted on the line indicated by the yellow line below the x-axis.